Unified Net Willans Line Model for Estimating the Energy Consumption of Battery Electric Vehicles

Candy Y. Li

Thesis submitted to the Faculty of the

Virginia Polytechnic Institute and State University

in partial fulfillment of the requirements for the degree of

Masters of Science

in

Mechanical Engineering

Douglas J. Nelson, Chair

Scott T. Huxtable

Zheng Li

August 11, 2022

Blacksburg, Virginia

Keywords: Battery Electric Vehicles, Energy Consumption Modeling, Unified Modeling, Willans Line, Vehicle Modeling

Unified Net Willans Line Model for Estimating the Energy Consumption of Battery Electric Vehicles

Candy Y. Li

(ABSTRACT)

Due to increased urgency regarding environmental concerns within the transportation industry, sustainable solutions for combating climate change are in high demand. One solution is a widespread transition from internal combustion engine vehicles (ICEVs) to battery electric vehicles (BEVs). To facilitate this transition, reliable energy consumption modeling is desired for providing quick, high-level estimations for a BEV without requiring extensive vehicle and computational resources. Therefore, the goal of this paper is to create a simple, yet reliable vehicle model, that can estimate the energy consumption of most, if not all, electric vehicles on the market by using parameter normalization techniques. These vehicle parameters include the vehicle test weight and performance to obtain a unified net Willans line to describe the input/output power through a linear relationship. A base model and three normalized models are developed by fitting the UDDS and HWFET energy consumption test data published by the EPA for all BEVs in the U.S. market. Out of the models analyzed, the normalization with weight performs best with the lowest RMSE values at 0.384 kW, 0.747 kW, and 0.988 kW for predicting the UDDS, HWY, and US06 data points, respectively, and 0.653 kW for all three data sets combined. Consideration of accessory loads at 0.5 kW improves the model normalized by weight and performance by a reduction of over 20% in RMSE for predictions with all data sets combined. Removing outliers in addition to consideration of accessory loads improves the model normalized by weight and performance by a reduction of over 36% in RMSE for predictions with all data sets combined. Overall,

results suggest that a unified net Willans line is largely achievable with accessible energy consumption data on U.S. regulatory cycles.

Unified Net Willans Line Model for Estimating the Energy Consumption of Battery Electric Vehicles

Candy Y. Li

(GENERAL AUDIENCE ABSTRACT)

Due to increased urgency regarding environmental concerns within the transportation industry, sustainable solutions for combating climate change are in high demand. One solution is a widespread transition from conventional internal combustion engine vehicles (ICEVs) to battery electric vehicles (BEVs). To facilitate this transition, reliable energy consumption modeling is desired to support quick, high-level analyses for BEVs without requiring expensive resources. Therefore, the goal of this paper is to create a simple vehicle model that can estimate the energy consumption of most, if not all, electric vehicles by scaling the data using vehicle parameters. These parameters include the vehicle test weight and performance to obtain a unified net Willans line model describing the input/output power through a linear relationship. The UDDS (city) and HWFET (highway) energy consumption data points used to develop the model are easily accessible from published EPA data. Out of the models analyzed, the normalization with test weight performs best with the lowest error values at 0.384 kW, 0.747 kW, and 0.988 kW for predicting the UDDS, HWFET, and US06 (aggressive city/highway cycle) data points, respectively, and 0.653 kW for all three data sets combined. Consideration of accessory loads at 0.5 kW improves the model normalized by weight and performance by a reduction of over 20% in error for predictions with all data sets combined. Removing outliers in addition to consideration of accessory loads improves the model normalized by weight and performance by a reduction of over 36% in error for

predictions with all data sets combined. Overall, results suggest that a unified net Willans line is largely achievable with accessible energy consumption data on U.S. regulatory cycles.

Acknowledgments

I would like to express my sincerest gratitude to Dr. Douglas J. Nelson for his invaluable guidance and patience as my professor, committee chair, and faculty advisor. His exceptional expertise and feedback has been significant from the beginning of my undergraduate studies until graduate school, and I could not have completed this journey without his support. I also greatly appreciate Dr. Scott T. Huxtable and Dr. Zheng Li for kindly taking the time to join my defense committee and review my final paper. Furthermore, this work would not have been possible without the generous funding support from the Virginia Tech Mechanical Engineering Department and the U.S. Department of Energy EcoCAR Mobility Challenge.

I'd also like to extend my gratitude to Cathy Hill and the Virginia Tech Graduate School for answering my countless questions and providing much needed clarity during times of uncertainty. I also wish to thank Justin Wu for his meaningful friendship, belief in my abilities, and unwavering support throughout this entire endeavor. Furthermore, I'd like to give a special thanks to Ryan Voltz for all his insightful suggestions, inspiration, and emotional support that helped carry this project until the end.

Finally, I am indebted to my friends and family for their continued support and encouragement. Especially my mother Yuzhu Yuan for her countless sacrifices to provide me the opportunity to attend college and follow my goals and aspirations.

This work was partially funded by support from the U.S. Department of Energy EcoCAR Mobility Challenge.

Contents

List of Figures

List of Tables

Chapter 1

Introduction

As the automotive industry addresses critical sustainability and environmental concerns, electric vehicles (EVs) are beginning to revolutionize modern day transportation. The transition to EVs is not a surprise since the automotive community has long understood the benefits of utilizing an electric powertrain over conventional internal combustion engine vehicles (ICEVs) [9]. For instance, the energy used to power electric vehicles can be sourced from renewable and cleaner sources without using fossil fuels [9]. Additionally, the tank to wheel (TTW) efficiency of an EV is significantly higher than gasoline ICEVs, which is estimated to be 11-27% compared to 50-80% estimated for EVs [2]. Due to the clear limitation in energy efficiency for an ICEV, greater emphasis on transitioning to EVs is considered as a desirable solution for combating modern environmental concerns. With the support of government regulation and automotive manufacturers in the United States, the total EV inventory is expected to increase 50 times by 2035 compared to the inventory in 2018 [17]. To achieve the desired rapid growth of EVs, the associated costs with transitioning could cost over 25% more than continuing the use of ICEVs during the projected period from 2015 to 2035 [16]. Therefore, tools like vehicle modeling can have incredible valuable in alleviating the costs associated with the increase in resources for the transition to EVs. Using modeling techniques, technological developments could arise quicker, cheaper, and with greater convenience compared to conducting physical tests on a vehicle.

1.1 Existing Vehicle Models

Current literature discusses two main types of vehicle models, physics models developed from an understanding of the vehicle dynamics, and data-driven models developed from identifying patterns in real-world data [11]. The vehicle dynamics are generally determined by calculating the tractive power required at the wheels to meet drive cycle demand [11]. A simple but popular method for vehicle modeling is based on a linear transfer function known as a Willans line as demonstrated by Rizzoni et al. [19] for both ICE and EV systems of a hybrid electric vehicle. These simplifications allow for vehicle analysis without significant computational resources.

On the other hand, fully data-driven models that are used to identify patterns within collected data can be computationally expensive to develop. Typically, these models utilize artificial neural networks that require large sets of data collected in real-world conditions for model training purposes in order to prevent bias. However, there are some benefits of using a data-driven model, including the fact that they typically self-adapt to a wide variety of different conditions without additional information on the external factors [11]. However, the significant time and resources needed to simply begin developing a data-driven vehicle model suggests that this method of modeling is not ideal for this study.

1.2 Study Objectives

The objective of this study is to develop a simple and efficient model for estimating the energy consumption for a wide array of BEVs. Therefore, the base EV model is adapted from a power-based physics model discussed by Harvey and Nelson [7] to summarize the vehicle dynamics and bi-directional power flow seen in EVs. The model utilizes elements

from the previously mentioned Willans line to create individual fits for an array of BEVs. For EV applications, the inverse slope of the Willans line model is referred as the marginal efficiency of the powertrain, which represents how much tractive power is achieved from a unit increase in battery power. Offsets in the linear relationship are attributed to accessory loads and losses in the vehicle. Additionally, Harvey and Nelson [7] propose a model created from the net tractive power and net battery energy consumption as a reliable method for estimating the energy consumption for UDDS and HWFET drive cycles within a 1% error and 4% for the US06 cycle.

Simple BEV models such as the one developed by Harvey and Nelson [7] are highly sought after, as they potentially remove barriers to entry in obtaining critical energy consumption data on multiple vehicles at once. For instance, teams that lack vehicle testing resources can still participate in automotive development. Furthermore, simplified models can be used to create unified models that can apply to many electric vehicles. Unified vehicle modeling is especially beneficial for offering more accessible research opportunities and faster progress on vehicle development. Applications may include modern control and energy management strategies like eco-driving, eco-routing, range estimation, and charge planning [11].

Therefore, the goal of this study is to develop a unified model for estimating the energy consumption of BEVs that can serve as a simple method for different vehicles without extensive computational and physical resources. Similar research has been conducted by Phlips and Scholl [12] [13] for conventional vehicles, which uses parameter normalization techniques to achieve a unified line. Additionally, a follow up study from Phlips also aims to achieve a unified BEV model [14]; however, the previously mentioned normalization techniques are not applied to the model. Therefore, this study will apply and analyze the normalization techniques for 2022 model year BEVs sold in the U.S. using the vehicle weight and rated power as the normalization parameters of choice.

Chapter 2

Background

2.1 Battery Electric Vehicle Model

2.1.1 Tractive Effort Model

The battery electric vehicle (BEV) model includes a two-part process adapted from Harvey and Nelson [7] for calculating the vehicle tractive effort and power consumption. To determine the tractive effort, the power required to complete a given drive cycle is calculated by analyzing the dynamics for a particular vehicle. The total required tractive force F_{tr} is the summation of the grade force F_g, inertial force F_i, and road load forces F_{rl}, as described in Figure 2.1 and Equation 2.1.

$$F_{tr} = F_i + F_{rl} + F_g \tag{2.1}$$

The grade force is defined as the longitudinal component of the gravitational force F_{grav} in the direction of vehicle motion as defined in Equation 2.3.

$$F_{grav} = mg \tag{2.2}$$

$$F_g = mg \cdot \sin\theta \tag{2.3}$$

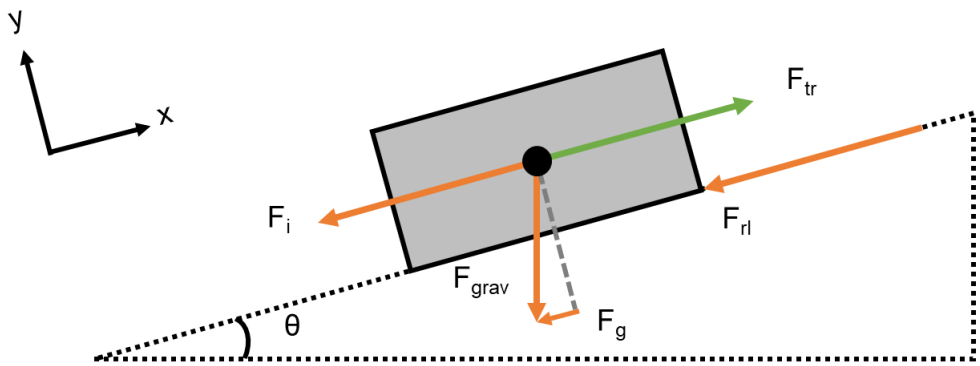

Figure 2.1: Free body diagram of the forces acting on a vehicle.

where $m\,[kg]$ is the test mass of the vehicle, $g\,[m/s^2]$ is the gravitational acceleration at $9.81\,[m/s^2]$ and θ is the angle of the road grade. The inertial force is equal to the force due to acceleration in addition to the inertia added by the vehicle's rotating components (wheels, tires, and driveline). The additional force due to inertia is approximated by an inertial factor, γ, with a value of 1.04 to represent the rotational inertia effects for modern vehicles as defined in Equation 2.4 [7] [20].

$$F_i = \gamma \cdot ma \tag{2.4}$$

where γ is the inertial factor and $a\,[m/s^2]$ is the acceleration of the vehicle. The aerodynamic drag and rolling resistance forces are summarized by a single road load force equation [1] that is approximated by three constant parameters A, B, and C, which are published in the EPA Test Car List data [6]. The provided units of these parameters are $[lbf]$, $\left[\frac{lbf}{mph}\right]$, and $\left[\frac{lbf}{mph^2}\right]$, respectively, which are converted to constants f_0, f_1, and f_2 with metric units for the following road load calculation.

$$F_{rl} = f_0 + f_1 \cdot v + f_2 \cdot v^2 \tag{2.5}$$

where $f_0\,[N]$ is the parameter that relates to the effects of rolling resistance, $f_1\left[\frac{N \cdot s}{m}\right]$ is the parameter that relates to the effects of rolling resistance as a function of the vehicle velocity, and $f_2\left[\frac{N \cdot s^2}{m^2}\right]$ is the parameter that relates to the aerodynamic drag effects on the vehicle.

Since the EPA provides drive cycle data at a sample rate of 1 Hz, the equations are modified to allow for discrete calculations. The velocity is averaged between each time step at the central value between two data points as shown in Equation 2.6. This method of discretization for the velocity allows for a more accurate representation of the dynamics that occur from one time step to the next. The acceleration is calculated as the change in drive cycle velocity divided by the time between each discrete step as presented in Equation 2.7. Similar to the calculation for v_{avg}, the angle of the grade is calculated by averaging the values between each data point as defined in Equation 2.8.

$$v_{avg}[n] = \frac{v[n+1] + v[n]}{2} \tag{2.6}$$

$$a[n] = \frac{v[n+1] - v[n]}{t[n+1] - t[n]} \tag{2.7}$$

$$\theta_{avg}[n] = \frac{\theta[n+1] + \theta[n]}{2} \tag{2.8}$$

where n represents the index of the discrete step of the calculated values, and $t\,[s]$ represents the drive cycle time at n. As a result, the discrete equations for the grade, inertial, and road load forces are rewritten as

$$F_g[n] = mg \cdot \sin\theta_{avg}[n] \tag{2.9}$$

$$F_i[n] = \gamma m \cdot a[n] \tag{2.10}$$

$$F_{rl}[n] = f_0 + f_1 \cdot v_{avg}[n] + f_2 \cdot v_{avg}[n]^2 \tag{2.11}$$

and the tractive power can be described discretely as

$$F_{tr}[n] = F_i[n] + F_{rl}[n] + F_g[n] \tag{2.12}$$

To obtain the tractive power for each time step, the tractive force is multiplied by the average velocity as illustrated in Equation 2.13

$$P_{tr}[n] = F_{tr}[n] \cdot v_{avg}[n] \tag{2.13}$$

where P_{tr} can be either a positive value depicted as P_{tr^+} to indicate that additional power is required to propel the vehicle to meet drive cycle demand, or a negative value depicted as P_{tr^-} to indicate that braking is required to slow down the vehicle to meet drive cycle demand. In the case that P_{tr} is 0, neither additional propulsion power or braking is needed to meet drive cycle demand. Often times, this condition is seen when the vehicle is idling at a stop or coasting. Once the tractive power is calculated for all time steps, the total or net energy required to meet drive cycle demand can be calculated using Equation 2.14, which is the discrete integral of the tractive power.

$$E_{tr}^{net} = \Sigma P_{tr}[n] \cdot \Delta t \tag{2.14}$$

where a summation is taken over the tractive power multiplied by the change in time Δt at each time step. Since the study uses 1 Hz data, the change in time is simply 1 second for each point, which simplifies the equation to be equivalent to the sum of the tractive power at each time step. Finally, the net tractive power of a drive cycle is obtained by dividing the

total energy required for a drive cycle by the total cycle time as shown below

$$P_{tr}^{net} = \frac{E_{tr}^{net}}{t_{cyc}} \tag{2.15}$$

where t_{cyc} represents the total drive cycle time. The average positive power $P_{tr^+}^{avg}$ and average negative power $P_{tr^-}^{avg}$ is also calculated using a similar method by determining the total drive cycle energy for each respective condition and dividing by the total drive cycle time. Therefore, the net tractive power for a drive cycle is also equal to the following equation,

$$P_{tr}^{net} = P_{tr^+}^{avg} + P_{tr^-}^{avg} \tag{2.16}$$

2.1.2 Powertrain Model

The remaining calculations are used to develop a powertrain model for determining the battery power required to complete a drive cycle. For this study, the powertrain model covers three possible powertrain states for a BEV: propulsion, regeneration, and idle. The propulsion state, as illustrated in Figure 2.2, refers to the condition where the powertrain provides positive tractive power to the wheels to propel the vehicle. This case includes coasting while the vehicle in motion, but not while the vehicle is idling. Additionally, the motor, inverter, and gearbox are combined into a single powertrain subsystem that follows a Willans line model with a defined marginal efficiency μ and offset. This offset describes the overhead losses associated with running the powertrain components, which is defined by P_{loss}. The accessory load P_{accy} is also present in the model because energy is supplied directly from the high voltage battery terminals to a DC/DC converter to power low voltage accessory components. In an ICEV, the accessory loads are not powered directly from the energy source, but rather an accessory belt connected to the powertrain. Therefore, the

accessory load is described separately from the powertrain subsystem. Additionally, since the regulatory drive cycle tests are conducted without climate control accessories, such as heating and cooling, these effects are not considered in this study.

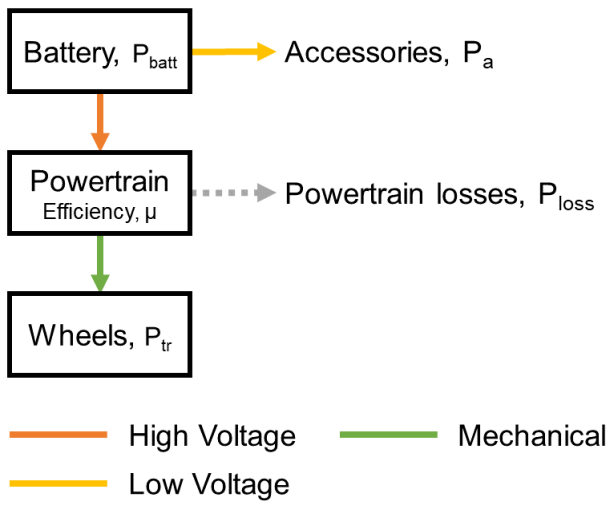

Figure 2.2: Power flow diagram of the BEV model in the propulsion state.

Therefore, the powertrain model during the propulsion state is described by Equation 2.17, where the positive tractive power P_{tr+} is multiplied by the inverse marginal efficiency and added to the powertrain offset losses and accessory loads. The inverse marginal efficiency is used because all equations are written in reference to the battery power. Additionally, the equation represents a backwards model that uses a known output of the Willans powertrain model to determine the input power. In Figures 2.2 and 2.3, the positive power flow is in the direction of the arrow. Connections are depicted as either mechanical or electrical, where the electrical connections are differentiated by low and high voltage.

$$\begin{aligned} P_{batt+} &= \frac{1}{\mu} P_{tr+} + P_{loss} + P_{accy} \\ if\, P_{tr}^{net} &\geq 0\, and\, idle = false \end{aligned} \tag{2.17}$$

where μ is the marginal efficiency of the powertrain system, P_{loss} is the fixed losses associated with the powertrain, and P_{accy} is the accessory loads for the vehicle.

The regeneration state refers to the condition where the vehicle must provide negative tractive power or braking to meet the drive cycle demand. Braking is largely comprised of two methods: friction braking and regenerative braking. Friction braking loses energy to the environment through heat, which cannot be recovered by the vehicle. However, regenerative braking provides negative tractive power by using the motor as a generator to recover energy that would have been lost by friction braking. Generally, BEVs blend the two sources of vehicle deceleration to optimize the desired vehicle behavior and efficiency while meeting required safety regulations [23]. Therefore, a regenerative braking fraction ρ is defined in Figure 2.3 to describe the ratio between the regenerated power over the total available braking power or negative tractive power. Note that the arrows in the plot represent the positive direction, so the tractive power at the wheels P_{tr} and battery power P_{batt} have negative values during this state. Another constraint on regenerative braking is the maximum

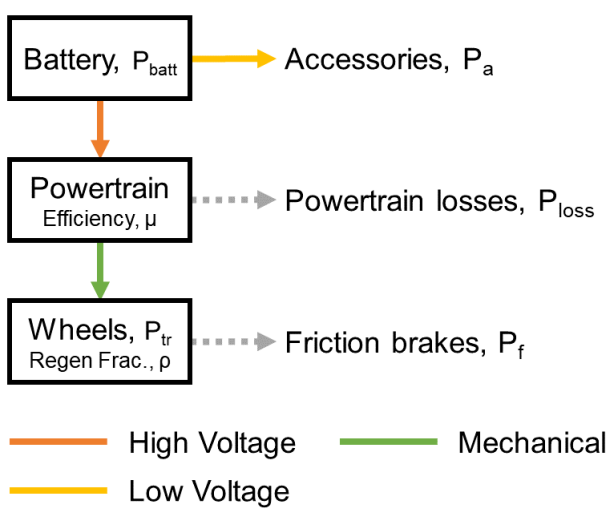

Figure 2.3: Power flow diagram of the BEV model in regeneration state.

braking power, which is used to limit the current going into the battery [22]. This value is approximately half the motor peak power as demonstrated by Rask et al. [15] and defined in Equation 2.18. Therefore, if the magnitude of the demanded negative tractive power is greater the max regenerative braking power, the powertrain model will only request the minimum of the two.

$$P_{max\,regen} = \frac{-P_{peak\,motor}}{2} \tag{2.18}$$

Additionally, it is possible to use the motor to provide negative tractive power at all speeds; however, this method is generally not preferred since regenerative braking at very low speeds requires more energy to run the motor compared to the regenerated energy [8]. Thus, a low-speed cut-off (LSCO) is defined at 5 mph to summarize all BEVs in the vehicle model [15]. If the vehicle speed reaches below the LSCO, the power available for regeneration is reduced to 0. The resulting equation for the regenerative braking power received by the powertrain is described in Equation 2.19.

$$\begin{aligned} P_{regen} &= \min\left(\|\rho \cdot P_{tr^-}\|, \|P_{max\,regen}\|\right) \\ &if\; v_{avg} < 5\,mph,\; P_{regen} = 0 \end{aligned} \tag{2.19}$$

where $P_{max\,regen}$ is the maximum regenerative power, $P_{peak\,motor}$ is the peak power of the vehicle powertrain, and, ρ is the regenerative fraction. As a result, the powertrain model during the regeneration state is defined as

$$\begin{aligned} P_{batt^-} &= \mu P_{regen} + P_{loss} + P_{accy} \\ &if\;\; P_{tr} < 0\,and\,idle = false \end{aligned} \tag{2.20}$$

where the available regenerative power is multiplied by the marginal efficiency μ. The powertrain losses and accessory loads are still added to the overall equation because both the powertrain and accessory components are active. Similar to the propulsion state, this

condition is not applicable when the vehicle is idle.

The final vehicle operation mode is idle mode, which describes conditions where the vehicle is turned on but not in motion. In this mode, the vehicle only draws power from the battery to operate accessory components. The powertrain is not active during this state; therefore, the demanded tractive power is 0. This equation differs from Equation 2.17 for calculating P_{batt^+} because the powertrain losses are not considered during idle. As such, the vehicle battery consumption during idle is described as follows

$$P_{batt^{idle}} = P_{accy} \tag{2.21}$$

As a result, the total battery power consumed can be described as

$$P_{batt} = P_{batt^+} + P_{batt^-} + P_{batt^{idle}} \tag{2.22}$$

Since the vehicle model is based off a net Willans line, the net consumption over a drive cycle is required for both the tractive power and battery power. Thus, following similar methods to Section 2.1.1, the discrete and net battery power equations are determined below.

$$P_{batt}[n] = P_{batt^+}[n] + P_{batt^-}[n] + P_{batt^{idle}}[n] \tag{2.23}$$

$$E_{batt}^{net} = \Sigma P_{batt}[n] \cdot \Delta t \tag{2.24}$$

$$P_{batt}^{net} = \frac{E_{batt}^{net}}{t_{cyc}} \tag{2.25}$$

The average positive power $P_{batt^+}^{avg}$, average negative power $P_{batt^-}^{avg}$, and average idle power $P_{batt^{idle}}^{avg}$ is also calculated by determining the total drive cycle energy for each respective condition and dividing by the total drive cycle time. Therefore, the net tractive power for a

drive cycle is also equal to the following equation,

$$P_{batt}^{net} = P_{batt^{+}}^{avg} + P_{batt^{-}}^{avg} + P_{batt^{idle}}^{avg} \tag{2.26}$$

2.1.3 Willans Vehicle Model

Individual Willans Model

The high-level vehicle model analyzed in this study follows a Willans line approach, which uses the energy consumption values for tractive power and battery power to create a linear fit. These values can be calculated using the tractive effort model in Section 2.1.1 or powertrain model in Section 2.1.2. An example Willans line model for a BEV is depicted in Figure 2.4, which is comprised of the discrete points for the tractive and battery powered using the previously mentioned models. These values are calculated from both the tractive effort model and powertrain model and not from actual EPA data. The data points in the green

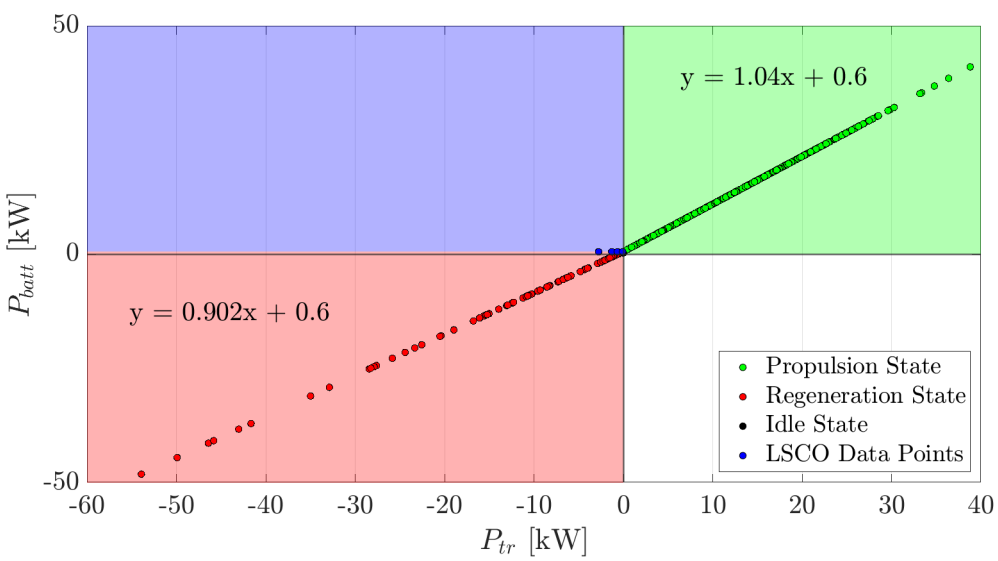

Figure 2.4: Example Willans line for a single BEV with propulsion, regeneration, and cutoff regions shown.

region represent the battery energy consumption in the propulsion state, while the data points in the red region represent the values in the regeneration state. The blue region represents conditions where negative tractive power is demanded at speeds below the LSCO; thereby disabling regenerative braking. Thus, the resulting battery consumption is equal to the powertrain offset losses and the accessory loads. For this example, both the offset losses and accessory loads are defined at 0.3 kW, which results in a positive battery consumption at 0.6 kW as illustrated by the blue points in Figure 2.5.

The regeneration region between the 0 kW battery power axis and the LSCO region includes the conditions where the regenerated power does not fully overcome the accessory and offset loads. However, the net battery power consumed is still less than the accessory and offset power, so regenerative braking is still worth utilizing. The black points at a battery consumption of 0.3 kW and tractive power of 0 kW represent the idle state, where the battery is only supplying energy to the accessories.

Finally, the slope for the data points in propulsion mode is equal to the inverse marginal efficiency, and the slope for the regeneration mode is equal to the marginal efficiency multiplied by the regenerative braking fraction. For this example, a marginal efficiency μ is set at 0.96, while the regenerative braking fraction ρ is set at 0.94, so the propulsion and regeneration slopes are 1.04 and 0.902, respectively.

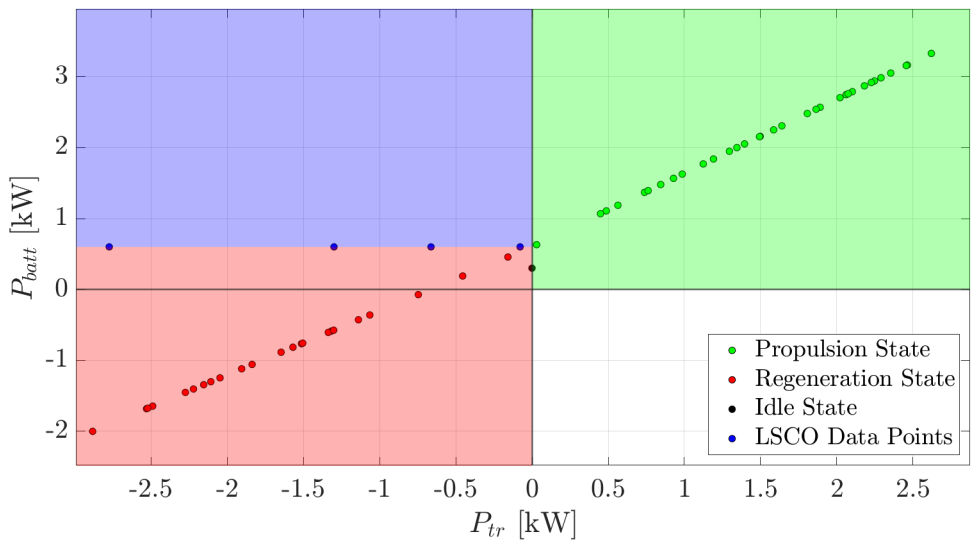

Figure 2.5: Zoomed-in plot of Figure 2.4 to illustrate LSCO effects on the propulsion/regeneration operation.

Net Willans Model

For the purposes of this study, a net Willans model is preferred since the net battery power is calculated using published data on vehicle fuel economy as discussed in Section 2.2.1. Often times, vehicle information required for more complex vehicle models is proprietary or difficult to obtain, which further encourages the use of a net Willans line model. In the U.S., fuel economy figures for the charge depleting (CD) UDDS (Urban Dynamometer Driving Schedule) and HWFET (Highway Fuel Economy Test) drive cycles are published in the EPA Test Car List (TCL) [6] data and the EPA Certificate Summary Information (CSI) reports in the Transportation and Air Quality Document Index System database [5] for all vehicles sold in the country. The tractive power is generally not provided in the published data; therefore, the value is calculated using the tractive effort model. As a result, each vehicle has at least two known energy consumption data points from published EPA data to create a net Willans line, which is used to predict additional data points. Occasionally, US06 energy consumption data is available, which consists of a drive cycle with more aggressive

characteristics with high acceleration for both city and highway driving.

For demonstration purposes, a net Willans line is shown in Figure 2.6 using the same example vehicle as Section 2.1.3. The UDDS, HWFET, and US06 energy consumption data points are calculated using the tractive effort and powertrain models. A linear fit is created using only the UDDS and HWFET data, and the US06 data is used as points to verify predictions in the model. Based on findings from Harvey and Nelson, the net Willans line model is capable of estimating the energy consumption of a US06 drive cycle within 4%, which is acceptable for high level analysis of a BEV [7]. This paper will define acceptability as a percent error within ±10%.

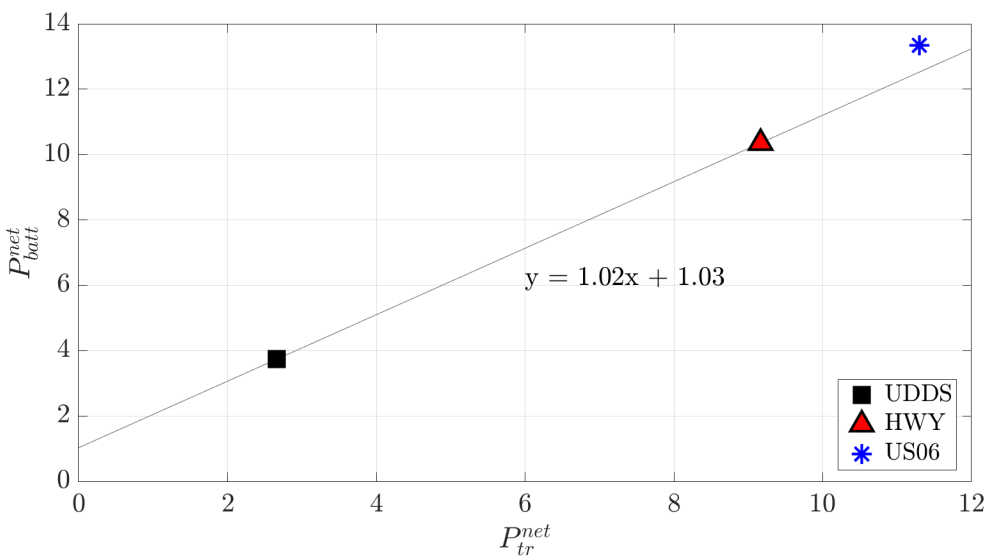

Figure 2.6: Net Willans line for an example BEV with a UDDS/HWFET linear fit and a measured US06 energy consumption data point.

The net Willans line in Figure 2.6 returns a slope of 1.02 and offset of 1.03 kW, which indicates that the BEV operates at a net marginal efficiency around 98%. Note that these values are not necessarily the same slope and offset as the previous powertrain Willans line in Figures 2.4 and 2.5, but rather a high level overview of the energy consumption that includes the effects of all powertrain states. Overall, the model estimates a net US06 battery

power consumption of 12.5 kW, while the actual value is 13.3 kW. Therefore, the percent error is about 6%, which meets the study's acceptability range. As a result, the net Willans line is chosen as the baseline model for investigating whether a unified BEV model can be achieved.

2.2 Sourcing Vehicle Data

2.2.1 EPA Test Car List Data

The electric vehicles analyzed in the study are gathered from the 2022 EPA Test Car List (TCL) data downloaded from the EPA's public website [6]. This set of data contains information such as the unadjusted miles per gallon equivalent (MPGe) fuel economy for the regulatory charge depleting UDDS and HWFET cycles. The listed MPGe value is a representation of the AC energy required to run the designated drive cycles compared to the energy used for a conventional ICEV, which assumes that a single gallon of gasoline is equivalent to 33.705 kWh in electrical power. Figure 2.7 highlights the fuel economy values for the UDDS and HWFET cycles listed in the TCL data plotted against the required tractive force determined by the tractive effort model. The specific vehicles used for analysis is detailed in Appendix A.

One observation of Figure 2.7 is that there are outliers with poor energy consumption values compared to other BEVs. However, closer inspection reveals that this difference is likely attributed to inconsistent units as those values are not within reasonable MPGe range for BEVs. Instead, the consumption values align with an alternative unit commonly used to display BEV energy consumption, kWh/100 mi. Therefore, to correct the different units, all data points under 60 MPGe are assumed to have units of kWh/100 mi and converted to

MPGe to obtain Figure 2.8.

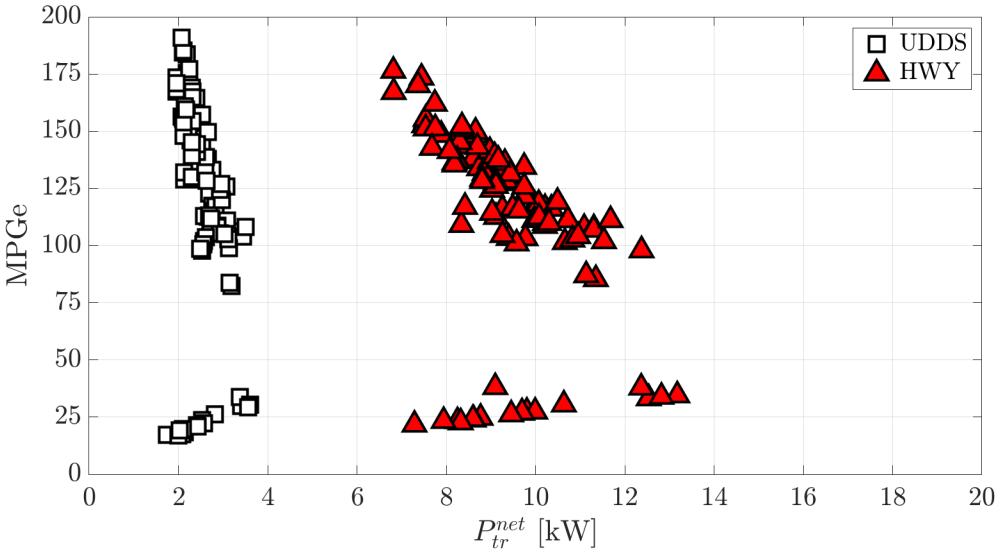

Figure 2.7: Raw MPGe data of electric vehicles listed in the EPA Test Car List data.

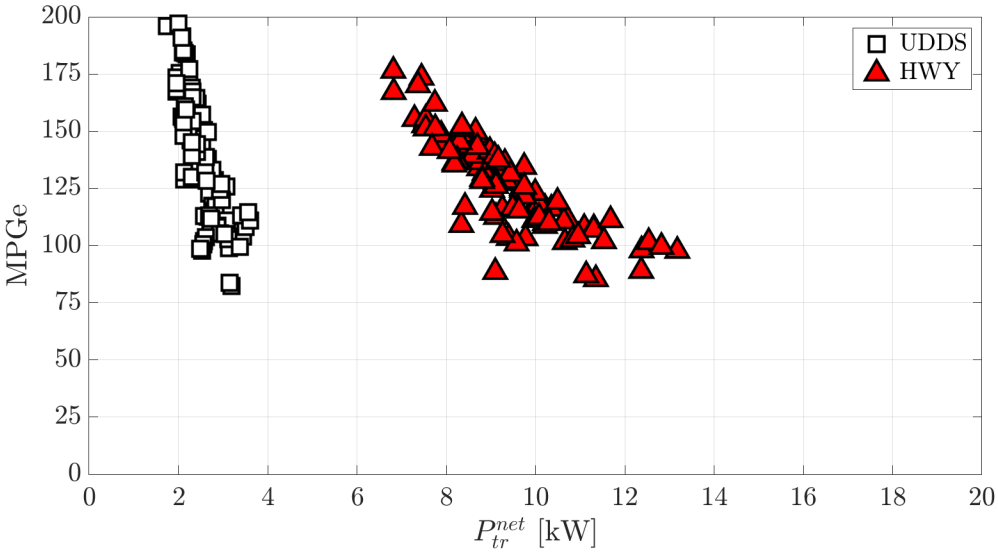

Figure 2.8: Corrected MPGe data of electric vehicles listed in the EPA Test Car List data.

Since the analysis in this study only considers battery consumption after the conversion from AC to DC energy, a charge efficiency η is used to find the available power after charging. This charge efficiency is considered in the calculation from MPGe to DC power as described

in Equation 2.27.

$$P_{DC\,Consumption} = \eta \left(\frac{1}{MPG_e}\right)\left(\frac{33.705\ kWh}{1\,gallon\,of\,gasoline}\right)\left(\frac{3600\,s}{1\,h}\right)\left(\frac{d_{cycle}}{t_{cycle}}\right) \tag{2.27}$$

where η represents the charging efficiency, MPG_e represents the fuel economy in miles per gallon equivalent, d_{cycle} is the total distance of the specified regulatory cycle, and t_{cycle} is the total time of the specified regulatory cycle. The DC power calculated from the TCL data is also equivalent to the net battery power P_{batt}^{net} used over a drive cycle. After finding the required DC power for each vehicle, the values are plotted against the cycle tractive power with an assumed charge efficiency of 87% as shown in Figure 2.9.

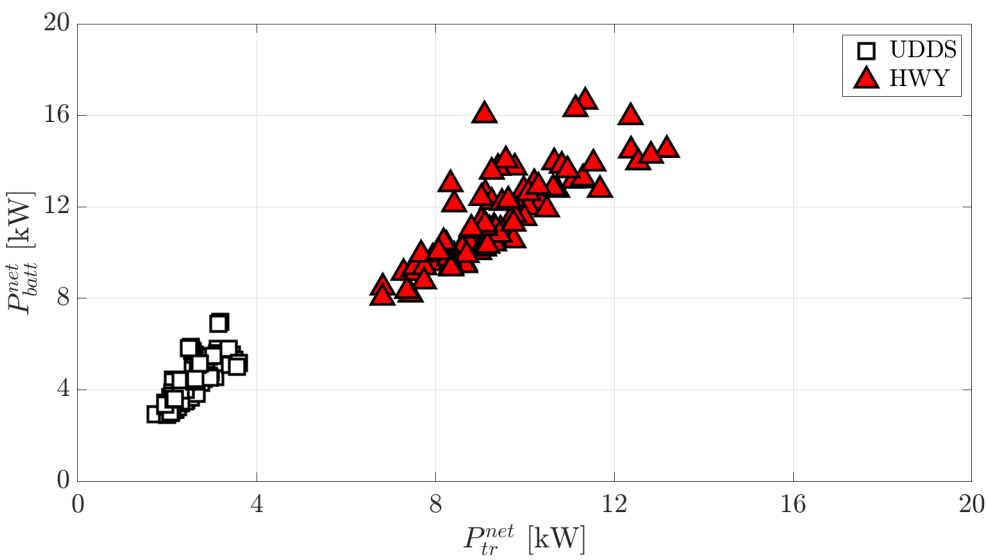

Figure 2.9: Calculated BEV DC energy consumption in EPA Test Car List data assuming $\eta = 87\%$.

2.3 Vehicles Chosen for Analysis

Table 2.1 is chosen for calculating individual charge efficiencies for more accurate analysis. These vehicles are chosen to represent the spread of the original data as well as popular car models on the market. Individual vehicle parameters are detailed in Appendix B.

Table 2.1: 2022 BEVs chosen from the EPA TCL data for analysis

Make	**Model**	**Description**	**Classification**
Rivian	R1S	Conserve Mode	Truck
Rivian	R1S	Sport Mode	Truck
Rivian	R1T	Conserve Mode	Truck
Rivian	R1T	Sport Mode	Truck
Chevrolet	Bolt EV		Car
Ford	Mustang Mach-E	AWD	Car
Ford	Mustang Mach-E	RWD	Car
Ford	Mustang Mach-E	AWD Extended Range	Car
Ford	Mustang Mach-E	RWD Extended Range	Car
Tesla	Model Y	AWD Performance	Car
Tesla	Model Y	AWD Long Range	Car
Tesla	Model Y	RWD	Car
Tesla	Model 3	RWD	Car
Tesla	Model 3	AWD Performance	Car
Tesla	Model 3	AWD Long Range	Car
Kia	EV6	AWD Long Range	Car
Kia	EV6	AWD Long Range	Car
Kia	EV6	RWD Long Range	Car
Nissan	Leaf	SV/SL, FWD	Car
Nissan	Leaf	FWD	Car
Lucid	Air Dream	Performance	Car
Hyundai	Kona Electric		Car
Audi	e-tron S		Truck
Mercedes	EQS 450+		Car
Porsche	Taycan	4S Perf Battery	Car

2.4 Estimating the Charge Efficiency

The charge efficiency is estimated by using known battery capacities released by the manufacturer or the DC energy consumption values found in the EPA Certificate Summary Information (CSI) report for the vehicle. These efficiencies are found by using Equation 2.28 or Equation 2.29 depending on the available information on the vehicle.

$$\eta = \frac{E_{DC,\,CD\,cycle}}{E_{AC,cycle}} \tag{2.28}$$

$$\eta = \frac{E_{batt\,cap,usable}}{E_{AC,cycle}} \tag{2.29}$$

where the numerator represents the DC energy consumed over a charge depleting cycle and the denominator represents the total AC energy used to recharge the vehicle after a charge depleting cycle. The usable battery capacity is assumed to be approximately the same value as the calculated DC energy consumption. If both the usable battery capacity and DC energy consumption for a charge depleting cycle are known, then the charge efficiency calculated from the DC energy consumption is used, as that information contains more significant values. Individual charge efficiencies and other vehicle parameters are detailed in Appendix B.

Using individual charge efficiencies yields the DC energy consumption versus tractive power plot shown in Figure 2.10. Overall, the battery consumption remains similar in value except for some vehicles, such as the Porsche Taycan 4S Performance Battery and Audi e-tron S. For instance, the Porsche Taycan has a calculated charge efficiency of 79% which shows lower DC battery consumption after charging losses than expected in Figure 2.10. Similarly, the Audi e-tron S has a calculated charge efficiency of 90%, which shows a higher DC battery consumption. Potential error in the charge efficiency calculations could be attributed to the

hardware in the vehicle, inaccurate data, or environmental conditions during the test that may affect charging losses.

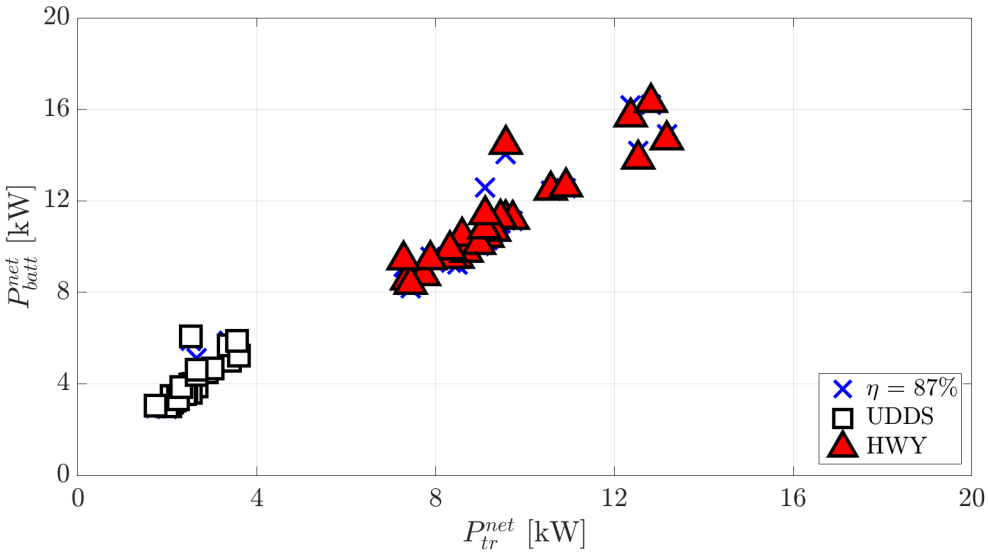

Figure 2.10: Comparison between estimating the charge efficiency at 87% and calculating the value.

Chapter 3

Normalized BEV Model

3.1 Net Willans Line Adaptation

The net Willans line modeling approach demonstrates energy consumption estimations of individual BEVs within a 1% error for UDDS and HWFET drive cycles and 4% for US06 drive cycles [7]. Since these values are below 10%, this strategy is considered a sufficient method for developing the base model for this study. Additionally, the convenience and functionality is particularly useful since substantial vehicle data or computational resources are not required to run energy consumption analysis. Therefore, the possibility of creating a unified net Willans line is desired to further reduce the resources needed to conduct vehicle analysis while maximizing the benefits of using a simplistic model. A normalization approach is taken to achieve a unified fit, which involves dividing the data points by a defined vehicle parameter and fitting the results.

Using data gathered in Appendix B for the chosen vehicles, the net tractive power P_{tr}^{net} is calculated by running the test mass and ABC road load coefficients through the tractive effort model discussed in Section 2.1.1. The net battery power P_{batt}^{net} is calculated by using Equation 2.27 and the published EPA fuel economy values listed in MPGe. Therefore, each vehicle has two data points for each drive cycle, which are used to create a single line fit that has individual slopes and offsets.

As a result, the net Willans lines for each chosen vehicle can be determined and plotted together as displayed in Figure 3.1. Without normalizing the model, the fitted lines already display similar net slopes in a linear pattern, where an increase in net tractive power is associated with a linear increase in net battery power. However, the vehicles do not line up perfectly due to varying net offset values.

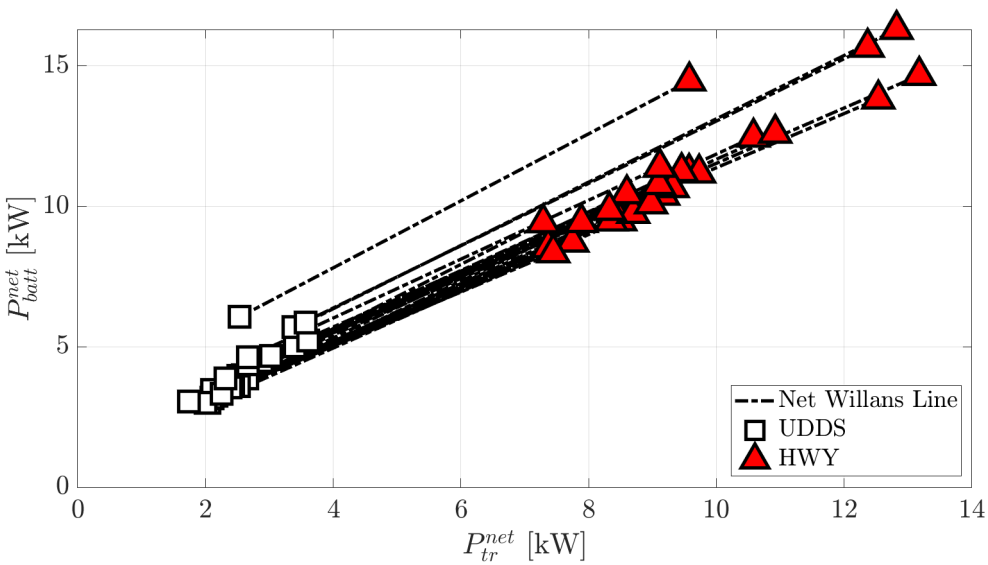

Figure 3.1: Individual net Willans lines plotted together for chosen vehicles listed in Appendix B

The offset in the net Willans line graph is expected to increase if a vehicle experiences greater average negative tractive power for a given drive cycle. For instance, a drive cycle that demands more negative tractive power will require more propulsive energy to result in the same net tractive power than a drive cycle that only uses the required propulsive power to meet the net tractive power. The reason is because EVs normally do not regenerate 100% of negative tractive energy back to the battery. As a result, the average negative tractive power of a drive cycle is recognized as a parameter that can skew a net Willans line model for a vehicle when fitting two different drive cycles. However, since modern EVs are assumed to have high regenerative fractions, this source of non-linearity may have little effect on the

overall fit and model estimations.

Therefore, a unified net Willans line model can still largely succeed in estimating the energy consumption at a high-level, especially since individual vehicle fits perform fairly well for estimating future data points [7]. To quantify whether this model is successful, an acceptable level of error to meet adequacy in this study is defined as a percent error within ±10% of the actual energy consumption.

3.2 Normalization

The normalization parameters chosen for the following analysis are adapted from studies conducted by Phlips [12] [13] that identify a unified net Willans line model for conventional vehicles. These parameters include the vehicle weight and performance, as defined by the power to weight ratio. Although ICEVs have different powertrain components, the theory remains similar for BEVs. For this study, the vehicle test weight, m, and the EV rated power to test weight ratio, P_{rated}/m, are used as the normalization parameters.

To create the normalized fit, the net tractive power, P_{tr}^{net}, is used on the x-axis and the net battery power, P_{batt}^{net}, is used on the y-axis of the model. The known input and output values of this model are then divided by the normalized parameter and fitted to a linear regression model created from the fitlm MATLAB function [10]. Statistics and other metrics on the linear model are also determined from the fitlm function.

The first parameter considered for normalization is the test weight of the vehicle, which increases the power required for a vehicle to overcome the inertial and road load forces [13]. Access to data required for this normalization is fairly easy to find given published EPA data. Following normalization, the resulting axes are P_{tr}^{net}/m for the x-axis and P_{batt}^{net}/m for

the y-axis.

The next normalization parameter is the performance of the vehicle, which is described by the vehicle rated power to test weight ratio, P_{rated}/m, and is also easily accessible in the EPA TCL data. The performance is chosen as a parameter because a motor does not have constant efficiency throughout its entire range of operation, similar to an ICEV. There are higher efficiency regions that may reach above 90% efficiency, but there are also regions that are much less at around 75% efficiency, especially at low speed and low torque operation [21]. One design factor that determines the powertrain operating points on a motor efficiency map within a drive cycle is the size of the motor. If a vehicle requires a very low or very high fraction of the motor rated power to overcome tractive forces, which are highly influenced by the weight of the vehicle, the efficiency may be lower than the average BEV. Vehicles designed for performance may fall under the category where the powertrain is oversized for the average use. As a result, performance is considered as a parameter for the normalization process, which results in $P_{tr}^{net}/(P_{rated}/m)$ for the x-axis and $P_{batt}^{net}/(P_{rated}/m)$ for the y-axis.

The final normalization involves combining the previous two vehicle parameters, weight m and performance P_{rated}/m, to receive the benefits of both normalization steps. The weight terms cancel out as described in Equation 3.1, which leaves the rated power P_{rated} as the remaining parameter as described below for the normalization. Therefore, the resulting axes are P_{tr}^{net}/P_{rated} for the x-axis and P_{batt}^{net}/P_{rated} for the y-axis.

$$\frac{P_{tr}^{net}/m}{P_{rated}/m} = \frac{P_{tr}^{net}}{P_{rated}}$$
$$\frac{P_{batt}^{net}/m}{P_{rated}/m} = \frac{P_{batt}^{net}}{P_{rated}} \tag{3.1}$$

3.2.1 Identifying the Base Model

The base model is created by fitting the UDDS and HWFET data points gathered from the EPA TCL data for vehicles listed in Appendix B. However, only select vehicles are listed in Table 3.1 to represent the vehicles displayed on the following plots for presentation purposes. Additionally, these are the only vehicles from Appendix B that include US06 energy consumption data. The corresponding net Willans line without any normalization is depicted in Figure 3.2.

Table 3.1: Condensed set of vehicles and parameters used for presenting normalization

Vehicle Name	(UDDS) P_{tr}^{net} [kW]	(UDDS) P_{batt}^{net} [kW]	(HWFET) P_{tr}^{net} [kW]	(HWFET) P_{batt}^{net} [kW]	P_{rated} [kW]	Test Weight [kg]
Rivian R1T Conserve	3.61	5.23	13.2	14.7	325	3175
Rivian R1T Sport	3.57	5.87	12.8	16.3	650	3175
Tesla Model Y AWD P	2.66	3.88	9.17	10.4	312	2154
Tesla Model 3 AWD P	2.52	3.60	8.70	9.75	321	1927
Tesla Model 3 AWD LR	2.10	3.18	7.45	8.35	293	1927
Lucid Air Dream P 21 in	2.32	3.86	7.89	9.43	828	2494
Mercedes EQS 450+	2.67	4.38	9.10	10.8	245	2721

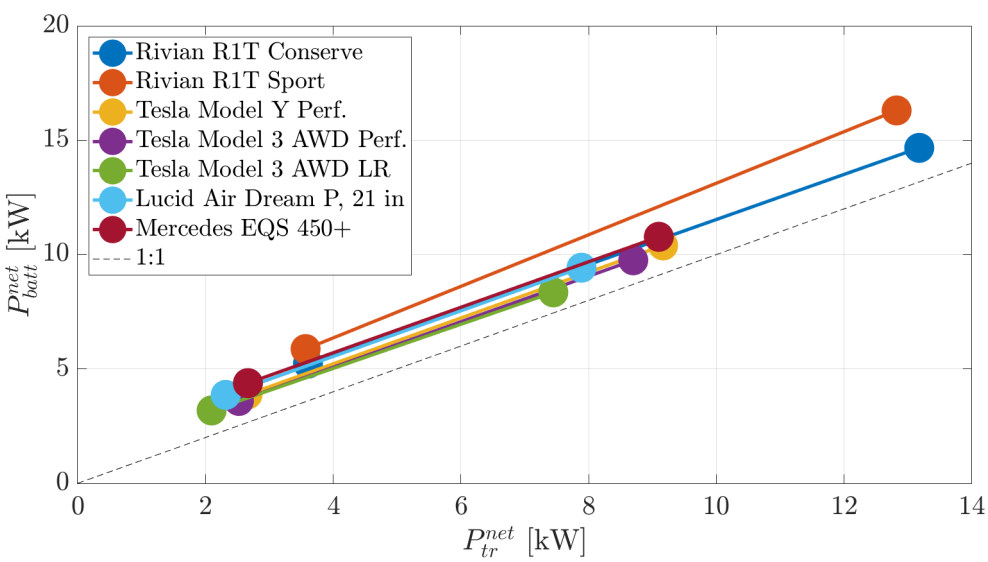

Figure 3.2: Base net Willans line without normalization.

Overall, the base model depicts the individual linear fits with similar slopes but differing offsets. These slopes range from 0.96 to 1.19 and offsets range from 0.84 kW to 3.04 kW.

Considering that the slope aligns with the inverse powertrain marginal efficiency, slopes less than 1 imply that the vehicle can achieve more output tractive power per unit of battery power. A slope less than 1 could be a result of fitting errors due to significant differences in regenerative braking between the UDDS and HWFET cycles, which would skew the linear fit. In this case, if the HWFET cycle recaptures a greater proportion of the available braking energy than the UDDS cycle, then the linear fit will be artificially biased towards a higher marginal efficiency and lower offset. This assumption is supported by the fact that the Rivian R1T Sport Mode shows a fairly different slope compared to the Conserve mode, where there is more aggressive regenerative braking [18]. Additionally, the Sport mode operates in all-wheel drive mode, which could imply different powertrain loss behavior.

Furthermore, the offset range between all vehicles is large, indicating differences in the overall power required to overcome road load forces and other previously mentioned factors, like regenerative braking, losses, and accessory loads. Overall, the vehicles with the highest energy consumption include the high performance and luxury vehicles, such as the Mercedes EQS 450+ and Rivian R1T in Sport mode. These vehicles may have higher accessory loads to run luxury features or greater losses due to more demanding performance requirements.

3.2.2 Normalizing by Weight

A large contributor to the overall tractive demand for any vehicle is the weight. As the weight of the vehicle increases, more energy is required to propel the vehicle forward, which is the same concept for ICEVs, HEVs, and BEVs [3]. Accordingly, the vehicle model is normalized by the equivalent test weight listed in the EPA TCL for the first normalized model.

The resulting normalization produces a collapsed graph for most of the vehicles. In Figure 3.3, the majority of the vehicles follow a similar slope and offset with the exception of

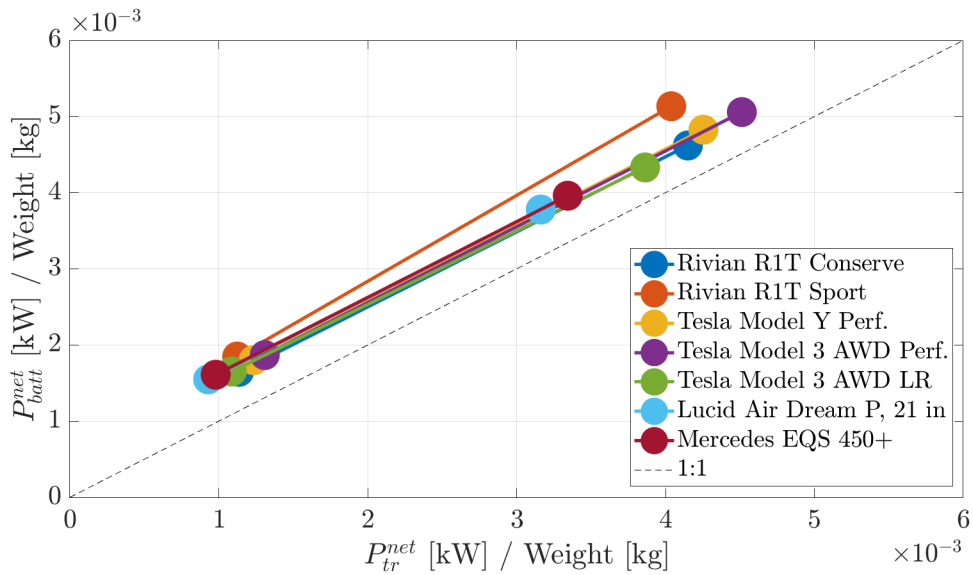

Figure 3.3: Net Willans line normalized by vehicle test weight.

the Rivian R1T in Sport Mode. Like the discussion in the previous section, this could be attributed to different amounts of regenerative braking during the HWFET cycle compared to the UDDS cycle. Additionally, the Sport Mode uses all-wheel drive instead of two-wheel drive in Conserve mode, which introduces greater overall losses as the number of moving components increase.

Another interesting observation of the model is how the UDDS data points collapse to a common region in the model. This behavior implies that the weight of the vehicle has greater influence on the energy consumption of the UDDS cycle compared to the HWFET cycle. The UDDS cycle also requires more acceleration, thus, more fraction of inertia power is needed to propel the vehicle. The assumption is further supported by Carlson et al. [3], who found that changes in mass had little impact on the overall energy consumption for the HWFET cycle compared to 2.4% to 4.1% change for a 10% increase in mass for the UDDS and US06 cycles.

3.2.3 Normalizing by Performance

The next normalization parameter investigated is the performance of the vehicle as defined by the rated power to test weight ratio, P_{rated}/m. This ratio is chosen to isolate the effects of operating at different efficiency regions for a given powertrain. For instance, a motor that requires low power to propel the vehicle in comparison to the total rated power is expected to experience lower efficiency. Since the UDDS and HWFET drive cycles have different peak power demands, the normalization potentially eliminates some of the losses associated with the vehicle architecture.

The resulting model from normalizing the performance parameter does not completely unify the net Willans lines; however, the data points for the Rivian R1T Sport Mode collapses closer to the rest of the data unlike the previous vehicle models. These changes suggest that the energy consumption for the R1T during Sport Mode is influenced more by the powertrain configuration and the vehicle does not operate in the most efficient regions when using all-wheel drive for the regulatory cycles. This idea is also supported by the examination that the R1T Conserve Mode collapses well with the rest of the net Willans lines from the other vehicles when half the listed rated power is used to represent the two-wheel drive mode.

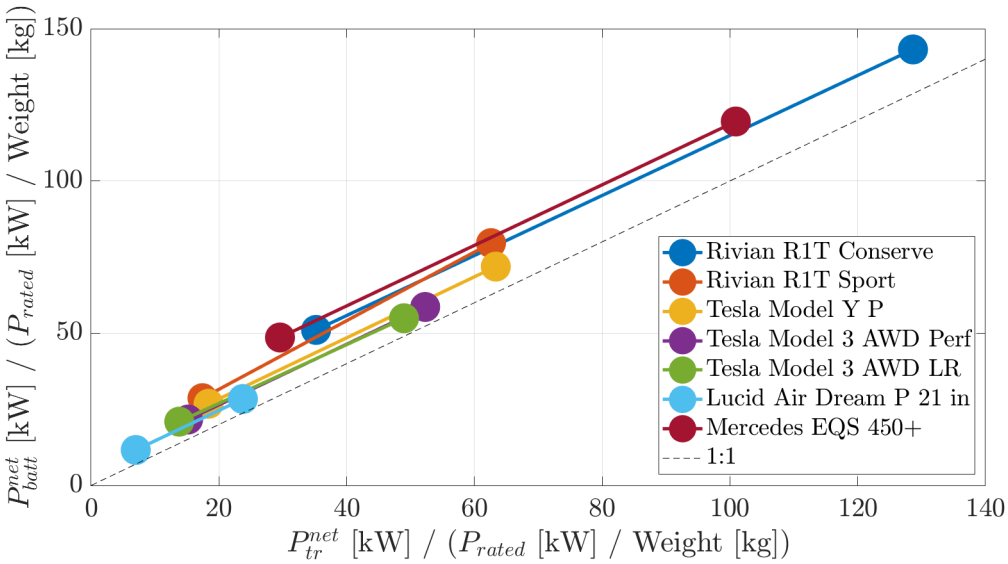

Figure 3.4: Net Willans line normalized by rated power to test weight ratio (performance).

3.2.4 Normalizing by Weight and Performance

The final normalization combines the previously discussed vehicle models and uses the weight and performance parameters. Since the weight terms cancel out, the resulting parameter is P_{rated}. Figure 3.5 indicates improvements in collapsing the UDDS and HWFET data points and results in similar slopes between the different vehicles. After this normalization step, the major remaining parameters affecting the offset for this model include the accessory loads, powertrain losses, and regenerative fraction. Since these values are not readily available to the public, further normalization is not considered for this study.

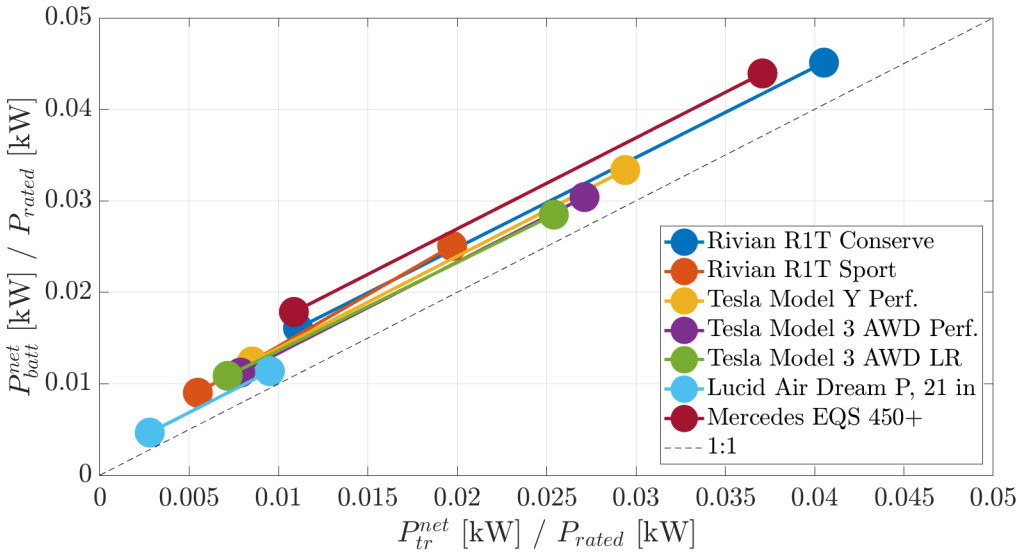

Figure 3.5: Net Willans line normalized by weight and performance.

Chapter 4

Results

4.1 Energy Consumption Estimation

4.1.1 Model Results - Base

The resulting base model is depicted in Figure 4.1, which shows a linear regression of the UDDS and HWFET data points for all chosen vehicles. In addition, the measured US06 energy consumption values from the EPA data and a 95% prediction interval is illustrated on the plot to visualize how close the linear model predicts measured values for other cycles. To quantify how well the base model and normalized vehicle model estimates the data, the root mean square error (RMSE) is calculated for each data set. As a baseline, Table 4.1 identifies the RMSE for fitting and predicting different sets of available data using the base model. Only the UDDS and HWFET energy consumption data is used for creating the line fits since US06 data is not always published by the EPA. However, if a vehicle containing published US06 energy consumption data is chosen, then that data point is included as way to verify model estimations. The list of chosen vehicles can be found in Appendix B.

Overall, the base model performs with a minimum RMSE of 470 W for predicting the UDDS energy consumption from a model fitted by UDDS points. A maximum RMSE of 1.1 kW is observed for estimating the US06 data points with a linear fit determined by the combined UDDS/HWFET data. Since the RMSE values appear to increase with drive

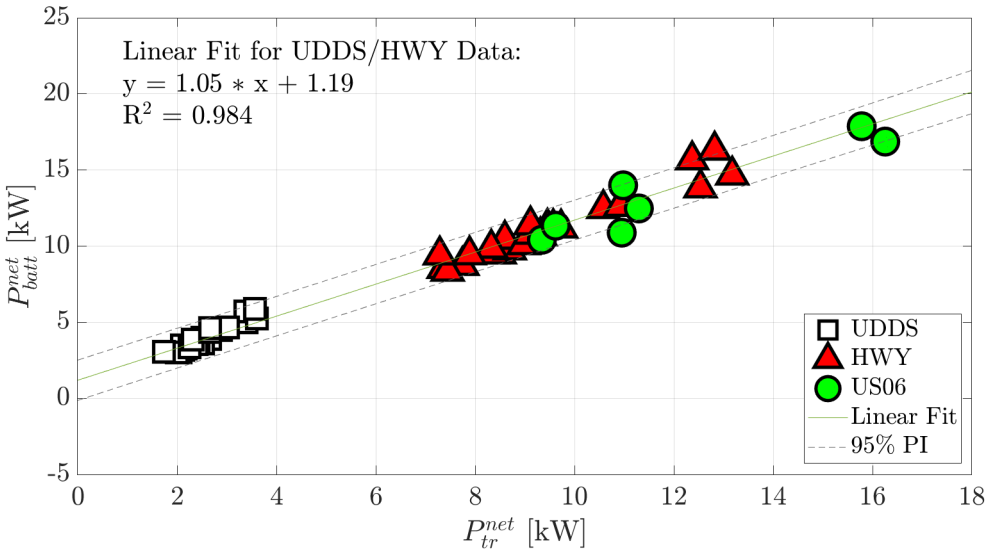

Figure 4.1: Base model for chosen vehicles listed in Appendix B.1

Table 4.1: RMSE for predicting energy consumption over different sets of fitted data points using the base model.

Fitted Data Points	**Predicted Data Points**	**RMSE [kW]**
UDDS	UDDS	0.470
HWFET	HWFET	0.818
UDDS/HWFET	UDDS	0.539
UDDS/HWFET	HWFET	0.862
UDDS/HWFET	US06	1.113
UDDS/HWFET	All	0.776

cycles containing higher net tractive powers, this pattern may suggest systematic error where possible relationships are not fully captured in the input/output model. Therefore, patterns in the error for the following sections are further observed to determine whether normalization reduces the error pattern. Ideally, the error values should appear random to demonstrate a sufficient model for describing the data.

Furthermore, the mean, min, and max percent error between the estimated and actual energy consumption is calculated for the different prediction fits as illustrated in Table 4.2. Without any normalization, the model performs fairly well with the mean percent error values under ±10%. However, the base model has a significant range in the minimum and maximum

Table 4.2: Percentage error for estimating the power consumption using the base model.

Data Fitted	**UDDS**	**HWFET**	**UDDS/HWFET**		
Data Predicted	**UDDS**	**HWFET**	**UDDS**	**HWFET**	**US06**
mean	1.1%	0.45%	0.1%	1.6%	4.8%
min	-34%	-22%	-35%	-21%	-8.0%
max	11%	7.9%	15%	9.4%	18%

predicted errors, where the greatest magnitude of error is -35%. Further observation of Table 4.3 reveals that the vehicle exhibiting the highest error is the Audi e-tron S. The P_{batt}^{net} estimated using the model is 3.94 kW, while the actual P_{batt}^{net} is just over 6 kW. Some differences noted in the Audi e-tron S is that the test weight and rated power to weight ratio are greater than the average value for other vehicles in the chosen list. Therefore, normalizing by these two values may help collapse the data points with high errors towards to other vehicle data.

Despite the large error for the Audi e-tron S, the majority of other vehicles in the chosen list have estimated percentage errors under 10% for the UDDS data. The predicted HWFET data points depict similar results with vehicles like the Audi e-tron S showing a percent error much higher than the rest of the data. Overall, the magnitude of error for the HWFET estimations are lower than the other predicted values for UDDS and US06, and all vehicles apart from the Audi e-tron S have estimated percent errors under 10%. Further details on the full percent error list can be accessed in Appendix D.

The predicted US06 data points yield a similar conclusion, where most vehicles show acceptable margins of error. Although the US06 energy consumption is not available for the Audi e-tron S, the Tesla Model 3 AWD P, a similar vehicle, also shows a trend of high percent error for the predicted values for all sets of data. For the US06 data points, only seven energy consumption data points are available from the chosen vehicles as displayed in Table 4.4. However, for the seven vehicles, the majority of the estimated values have errors within ±10%.

Table 4.3: Percentage error for estimating the UDDS power consumption with fitted UDDS/HWFET data using the base model.

Vehicle	**Estimated** $\mathbf{P^{net}_{batt}}$ **[kW]**	**Actual** $\mathbf{P^{net}_{batt}}$ **[kW]**	**% Error**
Rivian R1S Conserve	4.86	5.01	-3.1%
Rivian R1S Sport	4.83	5.69	-15.1%
Rivian R1T Conserve	5.07	5.23	-3.0%
Rivian R1T Sport	5.03	5.87	-14.3%
Chevrolet Bolt EV, Config 1	3.55	3.26	9.0%
Chevrolet Bolt EV, Config 2	3.55	3.26	9.0%
Ford Mustang Mach-E AWD	4.31	4.49	-4.0%
Ford Mustang Mach-E RWD	3.92	3.97	-1.4%
Ford Mustang Mach-E AWD ER	4.45	4.67	-4.6%
Ford Mustang Mach-E RWD ER	3.99	4.00	-0.1%
Tesla Model Y AWD P	4.07	3.88	4.9%
Tesla Model Y AWD LR	3.71	3.55	4.6%
Tesla Model Y RWD	3.44	3.01	14.5%
Tesla Model 3 RWD	3.50	3.18	10.1%
Tesla Model 3 AWD P	3.93	3.60	9.1%
Tesla Model 3 AWD LR	3.48	3.18	9.1%
Kia EV6 AWD LR 20 in	3.83	3.62	5.9%
Kia EV6 AWD LR 19 in	3.48	3.46	0.6%
Kia EV6 RWD LR	3.37	3.00	12.2%
Nissan Leaf SV/SL FWD	3.79	3.55	7.0%
Nissan Leaf FWD	3.64	3.33	9.2%
Lucid Air Dream P 21 in	3.71	3.86	-4.0%
Hyundai Kona Electric	3.10	3.04	1.9%
Audi e-tron S	3.94	6.06	-35.0%
Mercedes EQS 450+	4.08	4.38	-6.9%
Porsche Taycan 4S Perf Battery	4.08	4.62	-11.8%

Therefore, the base model appears to be adequate for the average BEV with the exception of a handful of vehicles that consistently have high percent error for all predicted sets of data. These vehicles appear to have higher vehicle weight and are considered ”performance” vehicles, which generally imply a higher power/weight ratio. Therefore, the following sections attempt to minimize outliers by normalizing the model by weight and performance parameters to collapse the Willans line fits to a single fit.

Table 4.4: Percentage error for estimating the US06 power consumption using the base model.

Vehicle	Estimated P_{batt}^{net} [kW]	Actual P_{batt}^{net} [kW]	% Error
Rivian R1S Conserve	18.45	16.87	9.4%
Rivian R1S Sport	17.95	17.88	0.4%
Tesla Model Y AWD P	13.21	12.48	5.9%
Tesla Model 3 AWD P	12.84	10.88	18.0%
Tesla Model 3 AWD LR	11.14	10.42	6.9%
Lucid Air Dream P 21 in	11.44	11.34	0.8%
Mercedes EQS 450+	12.87	13.99	-8.0%

4.1.2 Model Results - Weight

The first normalized parameter is the vehicle test weight since the tractive forces are highly dependent on the vehicle weight. The test weight is used instead of the curb weight of the vehicle since the data is related to the dynamometer tests where passenger and driver mass is added. After normalizing the model by weight, Figure 4.2 is produced with data points from each drive cycle noticeably shifted towards each other.

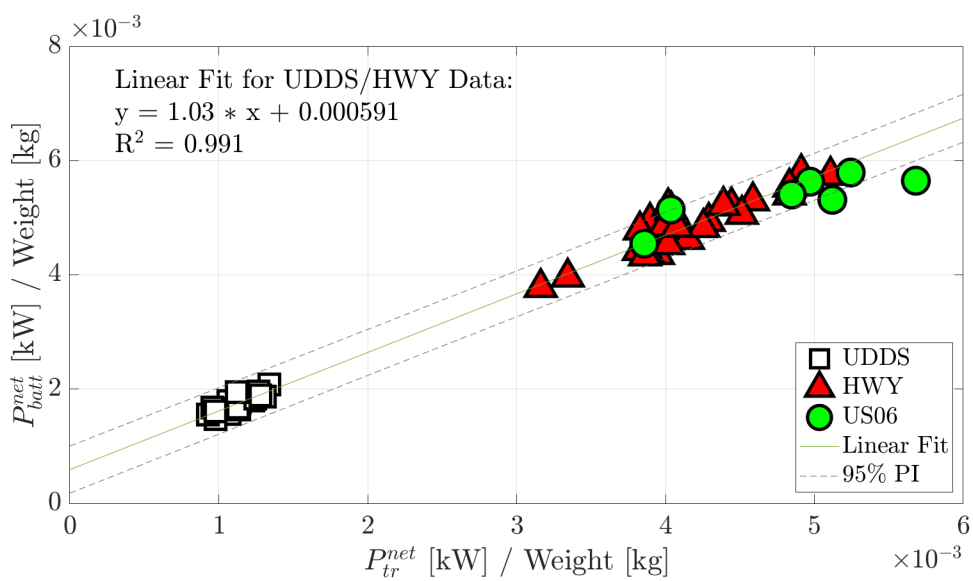

Figure 4.2: Model normalized by vehicle test weight for chosen vehicles listed in Appendix B

The net tractive power collapses horizontally in the model; however, variation in the battery

power between the different vehicles are still present. These results suggest that vehicle weight may not drastically affect the battery power as previously assumed. Furthermore, the prediction interval does not capture more data points than in the baseline model. In fact, a US06 data point falls outside of the bounds for the weight normalized model, unlike in the base model where the prediction interval captures all US06 points.

By observing the RMSE in Table 4.5, the error is slightly lower than the RMSE in the base model. Note that the model was normalized to different units, but the RMSE values have been converted back to kilowatts for comparison purposes. Despite the appearance of a less linear relationship observed in Figure 3.2.2, the RMSE values are lower than the ones observed for the base model. These results are further highlighted by the percent error, which is displayed in Table 4.6.

Table 4.5: RMSE in original units [kW] for predicting energy consumption over different sets of fitted data points using the model normalized by weight.

Fitted Data Points	**Predicted Data Points**	**RMSE [kW]**
UDDS	UDDS	0.358
HWY	HWY	0.697
UDDS/HWY	UDDS	0.384
UDDS/HWY	HWY	0.747
UDDS/HWY	US06	0.988
UDDS/HWY	All	0.653

Table 4.6: Summary of the estimation percent error for model normalized by test weight

Data Fitted	**UDDS**	**HWFET**	**UDDS/HWFET**		
Data Predicted	**UDDS**	**HWFET**	**UDDS**	**HWFET**	**US06**
mean	0.56%	0.31%	0.1%	-0.16%	3.6%
min	-23%	-16%	-35%	-19.52%	-7.6%
max	13%	8.3%	14.5%	7.1%	14%

Furthermore, the model fitted from the UDDS/HWFET data shows a decrease in the mean percent error. However, an observation of the individual percent errors in Table 4.7 for the predicted UDDS data points show that although the average error was reduced, some vehicles experience increased error compared to the base model.

Table 4.7: Percentage error for estimating the UDDS power consumption with fitted UDDS/HWFET data using the model normalized by weight.

Vehicle	Estimated P_{batt}^{net} [kW]	Actual P_{batt}^{net} [kW]	% Error
Rivian R1S Conserve	5.48	5.01	9.2%
Rivian R1S Sport	5.45	5.69	-4.2%
Rivian R1T Conserve	5.68	5.23	8.7%
Rivian R1T Sport	5.65	5.87	-3.8%
Chevrolet Bolt EV, Config 1	3.32	3.26	2.0%
Chevrolet Bolt EV, Config 2	3.32	3.26	2.0%
Ford Mustang Mach-E AWD	4.31	4.49	-4.1%
Ford Mustang Mach-E RWD	3.92	3.97	-1.1%
Ford Mustang Mach-E AWD ER	4.59	4.67	-1.8%
Ford Mustang Mach-E RWD ER	4.07	4.00	1.8%
Tesla Model Y AWD P	4.07	3.88	5.0%
Tesla Model Y AWD LR	3.73	3.55	5.0%
Tesla Model Y RWD	3.33	3.01	10.6%
Tesla Model 3 RWD	3.38	3.18	6.3%
Tesla Model 3 AWD P	3.79	3.60	5.4%
Tesla Model 3 AWD LR	3.36	3.18	5.4%
Kia EV6 AWD LR 20 in	3.84	3.62	6.2%
Kia EV6 AWD LR 19 in	3.50	3.46	1.3%
Kia EV6 RWD LR	3.33	3.00	10.7%
Nissan Leaf SV/SL FWD	3.66	3.55	3.4%
Nissan Leaf FWD	3.41	3.33	2.2%
Lucid Air Dream P 21 in	3.94	3.86	1.9%
Hyundai Kona Electric	2.92	3.04	-4.0%
Audi e-tron S	4.45	6.06	-26.6%
Mercedes EQS 450+	4.44	4.38	1.3%
Porsche Taycan 4S Perf Battery	4.22	4.62	-8.6%

In the base model, the Rivian R1S and R1T in Conserve Mode have a percent error of -3.1%, whereas they have a percent error of 9.2% in the normalized model. One possibility that might have affected these results is that these vehicles are the only chosen vehicles with two different modes for the same powertrain configuration. In Conserve mode, the Rivian vehicle only uses two motors, while the Sport Mode uses all four motors without changing the mass of the vehicle. Therefore, these data points might not be representative of all BEVs since not all vehicles have the same modes of operation.

In terms of estimating the US06 data points as shown in Table 4.8, most vehicles have an acceptable percentage error under ±10%. A major difference from this model compared

to the base model is that the percentage error for the Rivian R1S for both Conserve and Sport Mode are higher. Additionally, the Tesla Model 3 AWD P still exhibits high percent difference in the prediction, but the value is still improved from 18% to 14% error using this model.

Table 4.8: Percentage error for estimating the US06 power consumption using the model normalized by weight.

Vehicle	**Estimated** $\mathbf{P^{net}_{batt}}$ **[kW]**	**Actual** $\mathbf{P^{net}_{batt}}$ **[kW]**	**% Error**
Rivian R1S Conserve	18.61	16.87	10.3%
Rivian R1S Sport	18.13	17.88	1.4%
Tesla Model Y AWD P	12.90	12.48	3.4%
Tesla Model 3 AWD P	12.40	10.88	14.0%
Tesla Model 3 AWD LR	10.76	10.42	3.3%
Lucid Air Dream P 21 in	11.40	11.34	0.6%
Mercedes EQS 450+	12.93	13.99	-7.6%

In summary, the model fitted using the combined UDDS/HWFET data and normalized by vehicle test weight shows a moderate improvement in reducing the prediction error for UDDS, HWFET, and US06 data points.

4.1.3 Model Results - Performance

The next parameter used for normalization is the performance, which is defined as the ratio between the rated power and test weight, P_{rated}/m. The normalized model is depicted in Figure 4.3, which appears to follow a similar linear pattern like the base model, but the data is more spread out over the minimum and maximum axes values. Most of the data also seem to fall within the 95% prediction intervals.

Although the appearance of the model is more linear, the UDDS data points follow a slightly different slope compared to the HWFET data. Additionally, the RMSE values are greater than the previous models as detailed in Table 4.9.

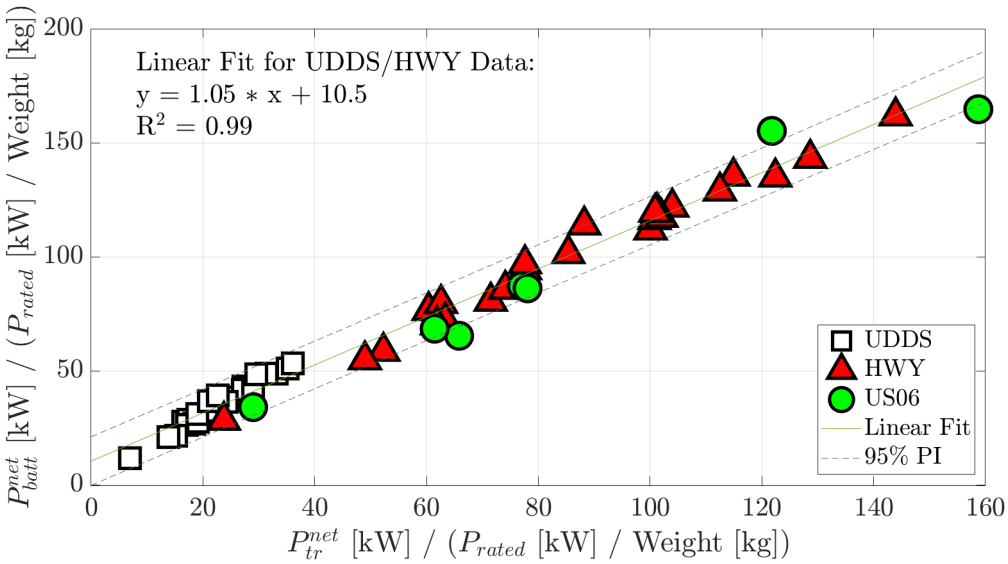

Figure 4.3: Model normalized by performance, P_{rated}/m, for chosen vehicles listed in Appendix B

Table 4.9: RMSE in original units [kW] for predicting energy consumption over different sets of fitted data points using the model normalized by performance.

Fitted Data Points	**Predicted Data Points**	**RMSE [kW]**
UDDS	UDDS	0.474
HWY	HWY	0.844
UDDS/HWY	UDDS	0.701
UDDS/HWY	HWY	0.943
UDDS/HWY	US06	1.708
UDDS/HWY	All	0.977

Similarly, the percent error values for each predicted set of data are higher than both the previously discussed models as depicted in Table 4.10. Overall, the predicted values for the US06 data points in Table 4.11 are mostly beyond ±10% for estimating energy consumption. Only the Rivian R1S and Tesla Model Y AWD P vehicles display percent errors under ±10%.

Table 4.10: Summary of the estimation percent error for model normalized by performance

Data Fitted	**UDDS**	**HWFET**	**UDDS/HWFET**		
Data Predicted	**UDDS**	**HWFET**	**UDDS**	**HWFET**	**US06**
mean	1.46%	0.97%	2.1%	2.21%	3.6%
min	-33%	-21%	-33%	-20.5%	-7.6%
max	16%	17.4%	60.5%	28.0%	14%

Table 4.11: Percentage error for estimating the US06 power consumption using the model normalized by performance.

Vehicle	Estimated P_{batt}^{net} [kW]	Actual P_{batt}^{net} [kW]	% Error
Rivian R1S Conserve	18.27	16.87	8.3%
Rivian R1S Sport	18.94	17.88	5.9%
Tesla Model Y AWD P	13.53	12.48	8.5%
Tesla Model 3 AWD P	13.41	10.88	23.2%
Tesla Model 3 AWD LR	11.56	10.42	10.9%
Lucid Air Dream P 21 in	13.89	11.34	22.5%
Mercedes EQS 450+	12.58	13.99	-10.1%

Therefore, normalizing the model by performance does not yield better performance than the base model or model normalized by weight. However, this model still demonstrates that the data points collapse horizontally, which may be useful in conjunction with another normalization parameter. Additionally, since the data points are spread out across the range of the model, there is less uncertainty about the linear fit between the UDDS and HWFET points.

4.1.4 Model Results - Weight and Performance

The final normalization step combines the weight and performance parameters and results in the model in Figure 4.4. Compared to the model normalized by performance, the data points in this model are more collapsed horizontally and vertically, and the linear fit contains data points that are evenly spaced across the entire range.

The data point on the far right of Figure 4.4 represents the standard Nissan Leaf, which suggests that the rated power of the vehicle is low compared to the net battery power and net tractive power. Alternatively, the data points to the far left for both the UDDS and HWFET data represent the Lucid Air Dream P, which has high rated power compared to the net battery power and net tractive power.

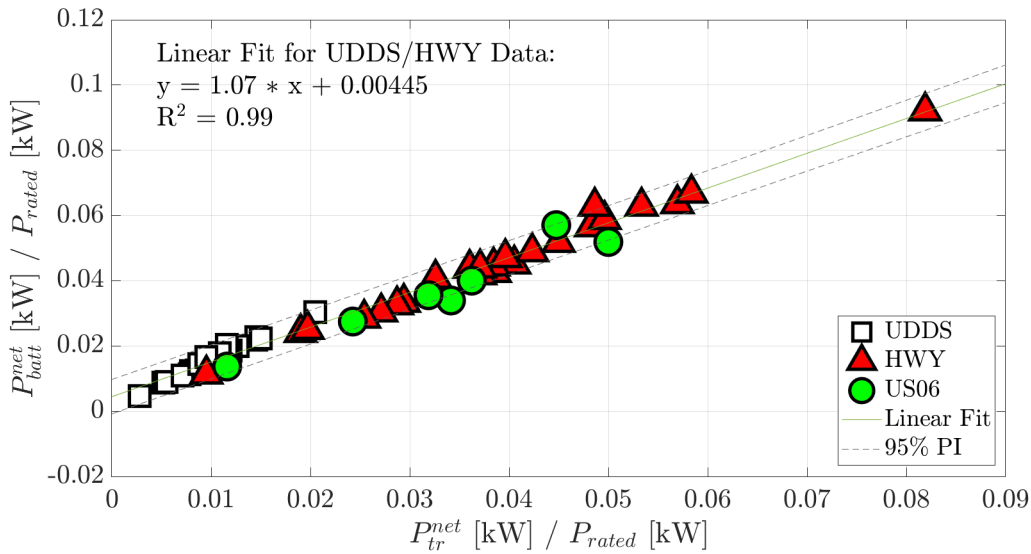

Figure 4.4: Model normalized by test weight and performance for chosen vehicles listed in Appendix B

Overall, the RMSE values observed for the vehicles in Table 4.12 show that the line fits created with individual drive cycle data perform better than the model created from fitting both UDDS and HWFET data. These findings suggest that there may be another parameter that differs between the UDDS and HWFET cycles, such as marginal efficiency. For instance, the efficiency of a motor is reduced when operating in regions with lower speeds, which may result in lower efficiency for the UDDS data compared to the HWFET data points. For the UDDS line fit, the normalized slope is 1.405, which corresponds to a normalized marginal efficiency of 0.71. For the HWFET line fit, the normalized slope is 1.101, which corresponds to a normalized marginal efficiency of 0.91. These values are only to demonstrate a difference in the slopes rather than the actual net efficiency, since that value may be skewed due to the normalization.

Similar findings are observed in Table 4.13, where the percent error values for the different sets of data are higher than the errors in the base model. Furthermore, the highest error for the combined UDDS/HWFET data is seen for the Lucid Air Dream P UDDS prediction at

Table 4.12: RMSE in original units [kW] for predicting energy consumption over different sets of fitted data points using the model normalized by weight and performance.

Fitted Data Points	**Predicted Data Points**	**RMSE [kW]**
UDDS	UDDS	0.456
HWY	HWY	0.779
UDDS/HWY	UDDS	0.721
UDDS/HWY	HWY	0.924
UDDS/HWY	US06	1.856
UDDS/HWY	All	1.007

Table 4.13: Summary of the estimation percent error for model normalized by weight and performance.

Data Fitted	**UDDS**	**HWFET**	**UDDS/HWFET**		
Data Predicted	**UDDS**	**HWFET**	**UDDS**	**HWFET**	**US06**
mean	1.2%	0.71%	1.4%	2.6%	11%
min	-31%	-20%	-26%	-17%	-8.3%
max	19%	16%	66%	31%	25%

66% error. However, this vehicle does not have overly high percent errors for the HWFET or US06 predictions, which may suggest that an element of vehicle operation during that state is not captured.

Table 4.14: Percentage error for estimating the US06 power consumption using the model normalized by weight and performance.

Vehicle	**Estimated P^{net}_{batt} [kW]**	**Actual P^{net}_{batt} [kW]**	**% Error**
Rivian R1S Conserve	18.81	16.87	11.5%
Rivian R1S Sport	19.86	17.88	11.1%
Tesla Model Y AWD P	13.48	12.48	8.1%
Tesla Model 3 AWD P	13.16	10.88	20.9%
Tesla Model 3 AWD LR	11.32	10.42	8.7%
Lucid Air Dream P 21 in	14.18	11.34	25.0%
Mercedes EQS 450+	12.83	13.99	-8.3%

For predicting the US06 energy consumption, the model performs fairly poorly with most percentages of error exceeding ±10%. However, the linear fit is able to capture data points fairly well, as the fit has the highest R^2 values as shown in Table 4.15. For this table, the intercept and RMSE are in their original units and show the results for both UDDS and

HWFET data points.

Table 4.15: Line fit results for each normalized model for linear regressions fitted with UDDS/HWFET fit points.

Normalized Parameters	**Slope**	**Intercept**	**R^2**	**RMSE**
-	1.06	1.26 [kW]	0.97	0.73 [kW]
m	1.02	6.3E-4 [kW/kg]	0.98	2.2E-4 [kW/kg]
P_{rated}/m	1.05	11.3 [kg]	0.98	5.73 [kg]
P_{rated}/m, m	1.06	4.8E-3 [-]	0.99	2.3E-3 [-]

4.2 Factoring Accessory Loads

As Harvey and Nelson [7] discusses, the net Willans line model is sensitive to accessory loads, which is not considered in the models above. Therefore, the models discussed still have the potential to perform with higher accuracy with further information on accessory loads. Since the accessory load is taken directly from the battery, as depicted in Figure 2.2, the load is subtracted from the net battery power before developing the model fit to obtain a better representation of the powertrain energy consumption.

A value of 0.5 kW is chosen to roughly represent the accessory loads of a vehicle during a dynamometer test [4]. The load is first subtracted from the net battery consumption to obtain new values for fitting the linear model for each normalization step. The x-y fitted values for the baseline model are as described below,

$$\begin{aligned} y\,(\text{fitted}) &= P_{batt}^{net} - 0.5\ \text{kW} \\ x\,(\text{fitted}) &= P_{tr}^{net} \end{aligned} \tag{4.1}$$

After the powertrain energy consumption is estimated from the model, the accessory load is

added to the result to obtain the final estimated net battery consumption.

By subtracting a load of 0.5 kW from the net battery consumption, the model normalized by performance and the model normalized by weight and performance both show improvements in the overall RMSE. Additionally, all normalized models show improvements in predicting US06 data points as depicted in Table 4.16. The RMSE for the predictions in the data set containing all data points decreases by over 20% for the model normalized by weight and performance. This model shows the highest improvement due to consideration of accessory loads; however, the model normalized by weight still has lower RMSE overall. Although the models fitted using only the UDDS and HWFET points show higher error when considering accessory loads, the changes are relatively small. The desired behavior is to reduce the error for estimated values for new data points that are not used to fit the model, such as the error for the US06 data points. Furthermore, since only a constant accessory load is used, information on the individual accessory loads for each vehicle can further improve the normalized model estimations.

Table 4.16: RMSE for normalized models after factoring a 0.5 kW accessory load in comparison to original models

		Normalization Type							
Fitted Data Points	**Predicted Data Points**	**Baseline [kW]**	**Change [%]**	**Weight [kW/kg]**	**Change [%]**	**Performance [kg]**	**Change [%]**	**Weight/ Performance [-]**	**Change [%]**
UDDS	**UDDS**	0.47	0%	0.39	7.9%	0.48	1.3%	0.46	1.4%
HWFET	**HWFET**	0.82	0%	0.71	2.5%	0.85	1.0%	0.79	1.1%
UDDS/HWFET	**UDDS**	0.54	0%	0.42	10.1%	0.58	-17.2%	0.55	-24.0%
UDDS/HWFET	**HWFET**	0.86	0%	0.79	5.4%	0.87	-8.2%	0.80	-13.2%
UDDS/HWFET	**US06**	1.11	0%	0.96	-2.8%	1.37	-19.8%	1.40	-24.6%
UDDS/HWFET	**All**	0.78	0%	0.68	4.0%	0.84	-14.3%	0.81	-20.1%

4.3 Removing Outliers

From observing Figure 3.1, which illustrates the individual net Willans lines for the chosen vehicles, the Audi e-tron S consumes more energy than the rest of the chosen vehicles. As

such, this vehicle may have characteristics that diverge from other BEVs that are not easily explained with published EPA data. Therefore, the outlier is removed from the data set to investigate whether the new model shows reduced error for the rest of the chosen vehicles. The same normalization steps are completed again using the new set of vehicles to develop new models.

As a result, removing the outlier vehicle significantly reduces the RMSE for all predicted values as depicted in Table 4.17. This model performs nearly as well as the original model that considers accessory loads in Section 4.2. In addition, when an accessory load of 0.5 kW is considered for the model without outlier data, the RMSE further reduces as indicated in Table 4.18. These results may suggest that the normalization steps alone are not able to isolate the vehicle differences of the Audi e-tron S. Furthermore, the accessory load may be significantly higher than the rest of the chosen vehicles. Since the powertrain losses and accessory loads are not readily available information, the reason for the outlier may be difficult to distinguish. Therefore, these results indicate that the performance of the model can be highly dependent on the set of vehicles used to create the model.

Table 4.17: RMSE results with outlier vehicle removed and compared to original model results when $P_{accy} = 0$

		Normalization Type							
Fitted Data Points	**Predicted Data Points**	**Baseline [kW]**	**Change [%]**	**Weight [kW/kg]**	**Change [%]**	**Performance [kg]**	**Change [%]**	**Weight/ Performance [-]**	**Change [%]**
UDDS	**UDDS**	0.23	-50.10%	0.21	-42.2%	0.22	-53.1%	0.21	-54.5%
HWFET	**HWFET**	0.54	-34.45%	0.51	-26.6%	0.54	-36.5%	0.49	-37.7%
UDDS/HWFET	**UDDS**	0.36	-33.10%	0.21	-46.0%	0.55	-21.9%	0.60	-16.8%
UDDS/HWFET	**HWFET**	0.60	-30.14%	0.51	-31.4%	0.70	-25.6%	0.74	-20.3%
UDDS/HWFET	**US06**	1.05	-6.05%	0.97	-2.2%	1.59	-6.9%	1.76	-5.1%
UDDS/HWFET	**All**	0.59	-23.73%	0.50	-23.6%	0.81	-17.0%	0.88	-12.5%

Table 4.18: RMSE results with outlier vehicle removed and compared to original model results when $P_{accy} = 0.5$ kW

		Normalization Type							
Fitted Data Points	**Predicted Data Points**	**Baseline [kW]**	**Change [%]**	**Weight [kW/kg]**	**Change [%]**	**Performance [kg]**	**Change [%]**	**Weight/ Performance [-]**	**Change [%]**
UDDS	**UDDS**	0.23	-50.10%	0.24	-31.6%	0.25	-46.4%	0.23	-50.2%
HWFET	**HWFET**	0.54	-34.45%	0.53	-23.4%	0.56	-34.2%	0.50	-35.7%
UDDS/HWFET	**UDDS**	0.36	-33.10%	0.24	-36.7%	0.40	-43.5%	0.38	-47.8%
UDDS/HWFET	**HWFET**	0.60	-30.14%	0.54	-27.5%	0.60	-36.7%	0.55	-40.5%
UDDS/HWFET	**US06**	1.05	-6.05%	0.94	-4.4%	1.26	-25.9%	1.31	-29.4%
UDDS/HWFET	**All**	0.59	-23.73%	0.51	-21.3%	0.65	-33.5%	0.64	-36.7%

Chapter 5

Conclusions

In summary, normalizing a net Willans line may serve as a simple and adequate model for estimating the energy consumption with only limited data published publicly by the EPA. Additionally, these models have high potential for improvement when accessory loads and powertrain losses are known.

The resulting RMSE for each normalized model fitted using the combined UDDS and HWFET data points is summarized by Figure 5.1. Similarly, the resulting RMSE for the models that consider accessory loads at 0.5 kW is detailed in Figure 5.2, which highlights improvements in the estimations.

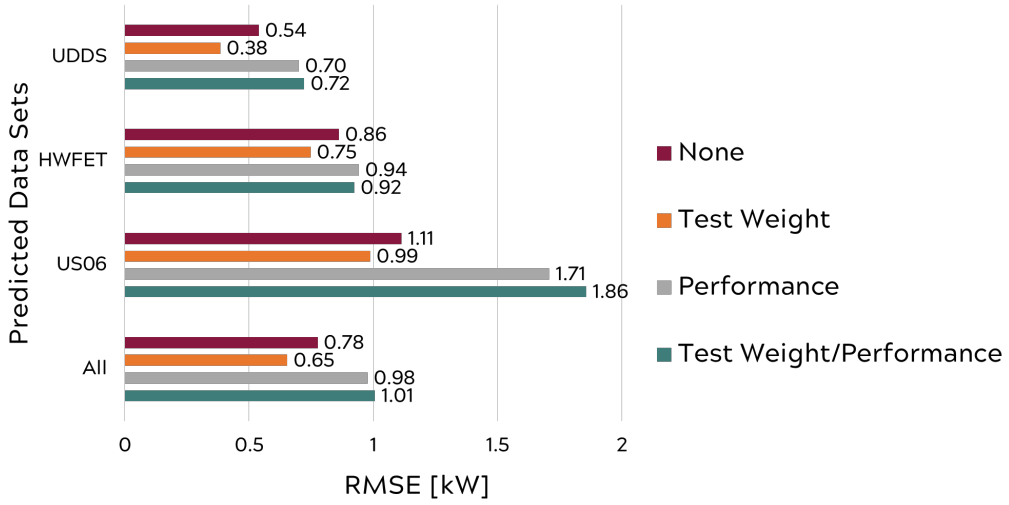

Figure 5.1: RMSE results for all normalization models for data sets estimated using a linear model fitted by both UDDS/HWFET data.

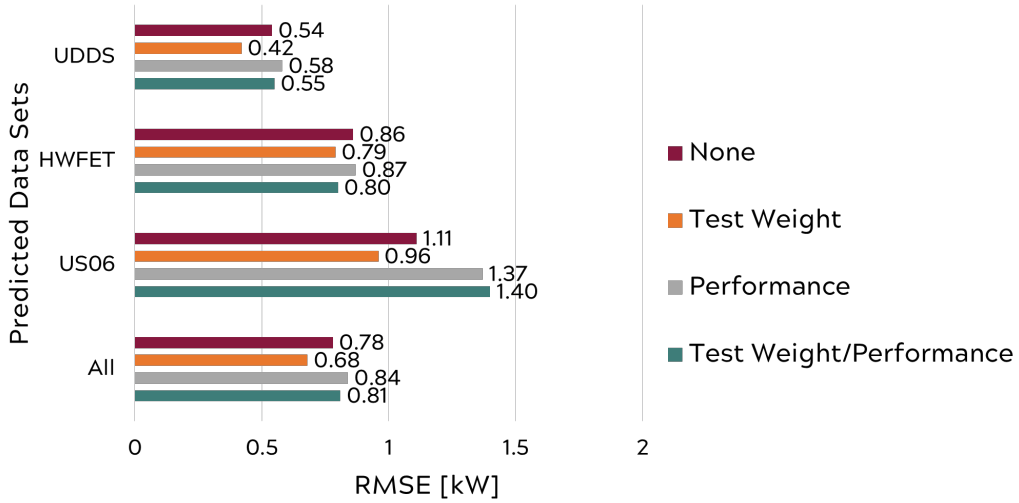

Figure 5.2: RMSE results for all normalization models for data sets estimated using a linear model fitted by both UDDS/HWFET data with considered 0.5 kW load

In brief, findings in this study include:

- A unified net Willans line in terms of the net tractive power, P_{tr}^{net}, and net battery power, P_{batt}^{net}, is largely successful for fitting regulatory cycles
- Normalizing a net Willans line by vehicle test weight yields improvements in the model predictions for UDDS, HWFET, and US06 data points
- Normalizing a net Willans line by performance collapses the data horizontally to achieve data points evenly scattered across the model range
- Normalizing a net Willans line by performance helps achieve similar net Willans line slopes across all vehicles
- Normalizing a net Willans line by vehicle test weight and performance produces the highest errors out of all the models analyzed in this study

- Despite large prediction errors, the model normalized by vehicle test weight and performance has the highest R^2 value
- The slope of the unified net Willans line is approximately the inverse of the powertrain marginal efficiency when variable terms other than P_{tr}^{net} are constant
- The offset of the unified net Willans line is approximately equivalent to the accessory loads and powertrain losses
- A more accurate unified net Willans line model is possible with further vehicle information on accessory loads and powertrain losses

Bibliography

[1] *Estimation of Road Load Parameters via On-road Vehicle Testing Tire Technology Expo 2013 February 5-7 Cologne Germany*, 2013. URL https://www.aandd.jp/support/dsp_papers/estimation.pdf.

[2] Aiman Albatayneh, Mohammad N Assaf, Dariusz Alterman, and Mustafa Jaradat. Comparison of the overall energy efficiency for internal combustion engine vehicles and electric vehicles. *Environmental and Climate Technologies*, 24:669–680, 2020. doi: 10.2478/rtuect-2020-0041. URL https://doi.org/10.2478/rtuect-2020-0041.

[3] Richard Barney Carlson, Henning Lohse-Busch, Jeremy Diez, and Jerry Gibbs. The measured impact of vehicle mass on road load forces and energy consumption for a bev, hev, and ice vehicle. *SAE International Journal of Alternative Powertrains*, 2:105–114, 2013. ISSN 21674191. doi: 10.4271/2013-01-1457.

[4] Richard Barney Carlson, Jeffrey Wishart, and Kevin Stutenberg. On-road and dynamometer evaluation of vehicle auxiliary loads. *SAE International Journal of Fuels and Lubricants*, 9(1):260–268, apr 2016. ISSN 1946-3952. doi: https://doi.org/10.4271/2016-01-0901. URL https://doi.org/10.4271/2016-01-0901.

[5] EPA. Epa's transportation and air quality document index system. Technical report, U.S. Environmental Protection Agency, 2022. URL https://dis.epa.gov/otaqpub/publist1.jsp.

[6] EPA. 2022 test car list data. Technical report, U.S. Environmental Protection Agency, 2022. URL https://www.epa.gov/system/files/documents/2022-04/22-tstcar-2022-04-15.xlsx.

[7] Dan Harvey and Douglas Nelson. Willans line bidirectional power flow model for energy consumption of electric vehicles. *SAE Technical Paper 2022-01-0531*, 2022. doi: 10.4271/2022-01-0531. URL https://doi.org/10.4271/2022-01-0531.

[8] Shoeib Heydari, Poria Fajri, Md Rasheduzzaman, and Reza Sabzehgar. Maximizing regenerative braking energy recovery of electric vehicles through dynamic low-speed cutoff point detection. *IEEE Transactions on Transportation Electrification*, 5:262–270, 3 2019. ISSN 23327782. doi: 10.1109/TTE.2019.2894942.

[9] Ingrid Malmgren. Quantifying the societal benefits of electric vehicles. *World Electric Vehicle Journal*, 8:996–1007, 2016. ISSN 2032-6653. doi: 10.3390/wevj8040996. URL https://www.mdpi.com/2032-6653/8/4/996.

[10] MathWorks. fitlm - fit linear regression model. URL https://www.mathworks.com/help/stats/fitlm.html.

[11] Ilyès Miri, Abbas Fotouhi, and Nathan Ewin. Electric vehicle energy consumption modelling and estimation—a case study. *International Journal of Energy Research*, 45:501–520, 2021. doi: https://doi.org/10.1002/er.5700. URL https://onlinelibrary.wiley.com/doi/abs/10.1002/er.5700.

[12] Patrick Phlips and David Scholl. Characterization of powertrain technology benefits using normalized engine and vehicle fuel consumption data. *SAE International Journal of Fuels and Lubricants*, 11:517–531, 4 2018. ISSN 1946-3952. doi: https://doi.org/10.4271/2018-01-0318. URL https://doi.org/10.4271/2018-01-0318.

[13] Patrick Phlips, William Ruona, Thomas Megli, and Mrudula Orpe. Unified power-based vehicle fuel consumption model covering a range of conditions. *SAE International Journal of Advances and Current Practices in Mobility*, 2:2320–2336, 4 2020. ISSN 2641-

9637. doi: https://doi.org/10.4271/2020-01-1278. URL https://doi.org/10.4271/2020-01-1278.

[14] Patrick Phlips, Thomas Megli, and William Ruona. Unified power-based analysis of combustion engine and battery electric vehicle energy consumption. *WCX SAE World Congress Experience*, 3 2022. ISSN 0148-7191.

[15] Eric Rask, Danilo Santini, and Henning Lohse-Busch. Analysis of input power, energy availability, and efficiency during deceleration for x-ev vehicles. *SAE International Journal of Alternative Powertrains*, 2:350–361, 4 2013. ISSN 2167-4191. doi: https://doi.org/10.4271/2013-01-1473. URL https://doi.org/10.4271/2013-01-1473.

[16] Jenny Riesz, Claire Sotiriadis, Daisy Ambach, and Stuart Donovan. Quantifying the costs of a rapid transition to electric vehicles. *Applied Energy*, 180:287–300, 2016. ISSN 0306-2619. doi: https://doi.org/10.1016/j.apenergy.2016.07.131. URL https://www.sciencedirect.com/science/article/pii/S0306261916310789.

[17] Nele Rietmann, Beatrice Hügler, and Theo Lieven. Forecasting the trajectory of electric vehicle sales and the consequences for worldwide co2 emissions. *Journal of Cleaner Production*, 261:121038, 2020. ISSN 0959-6526. doi: https://doi.org/10.1016/j.jclepro.2020.121038. URL https://www.sciencedirect.com/science/article/pii/S0959652620310854.

[18] Rivian. Drive modes | 8 modes, all terrains, one r1t. ride along, off-road and on, 2022. URL https://youtu.be/JN9lAJ0LiLw.

[19] G Rizzoni, L Guzzella, and B M Baumann. Unified modeling of hybrid electric vehicle drivetrains. *IEEE/ASME Transactions on Mechatronics*, 4:246–257, 1999. doi: 10.1109/3516.789683.

[20] Gino Sovran and Dwight Blaser. A contribution to understanding automotive fuel economy and its limits. *SAE Technical Paper 2003-01-2070*, 2003. doi: 10.4271/2003-01-2070. URL https://doi.org/10.4271/2003-01-2070.

[21] Sheldon S. Williamson, Ali Emadi, and Kaushik Rajashekara. Comprehensive efficiency modeling of electric traction motor drives for hybrid electric vehicle propulsion applications. *IEEE Transactions on Vehicular Technology*, 56:1561–1572, 7 2007. ISSN 00189545. doi: 10.1109/TVT.2007.896967.

[22] Takuya Yabe, Kan Akatsu, Nobunori Okui, Tetsuya Niikuni, and Terunao Kawai. Efficiency improvement of regenerative energy for an ev. *World Electric Vehicle Journal*, 5:494–500, 2012. ISSN 2032-6653. doi: 10.3390/wevj5020494. URL https://www.mdpi.com/2032-6653/5/2/494.

[23] Yixin Yao, Yanan Zhao, and Mark Yamazaki. Integrated regenerative braking system and anti-lock braking system for hybrid electric vehicles & battery electric vehicles. *SAE Technical Paper 2020-01-0846*, 2020. doi: 10.4271/2020-01-0846.

Appendices

Appendix A

EPA TCL Vehicle Data

The following table includes the list of BEVs in the 2022 EPA Test Car List data [6].

Table A.1: List of chosen vehicles and parameters from 2022 EPA TCL data

Make	Model	Vehicle Config #	Rated Power (HP)	ETW (lbs)	Test Procedure Description	FE (MPGe)	A (lbf)	B (lbf/mph)	C (lbf/mph^2)
Audi	Q4 e-tron 50	0	295	5250	Charge Depleting UDDS	141	32.642	0.32916	0.017693
Audi	Q4 e-tron 50	0	295	5250	Charge Depleting Highway	127.8	32.642	0.32916	0.017693
Audi	Q4 e-tron 50	1	295	5250	Charge Depleting UDDS	144.2	32.642	0.32916	0.017693
Audi	Q4 e-tron 50	1	295	5250	Charge Depleting Highway	126.1	32.642	0.32916	0.017693
AUDI	Audi e-tron 55 quattro Sportback	0	355	6000	Charge Depleting UDDS	103.6	35.745	0.38704	0.018042
AUDI	Audi e-tron 55 quattro Sportback	0	355	6000	Charge Depleting Highway	103.2	35.745	0.38704	0.018042
AUDI	Audi e-tron 55 quattro Sportback	1	355	6000	Charge Depleting UDDS	100.7	35.745	0.38704	0.016529
AUDI	Audi e-tron 55 quattro Sportback	1	355	6000	Charge Depleting Highway	103.3	35.745	0.38704	0.016529
AUDI	e-tron S	0	496	6500	Charge Depleting UDDS	97.7	35.362	0.26405	0.019776
AUDI	e-tron S	0	496	6500	Charge Depleting Highway	100.9	35.362	0.26405	0.019776
AUDI	e-tron S	1	496	6500	Charge Depleting UDDS	98.7	35.362	0.26405	0.018508
AUDI	e-tron S	1	496	6500	Charge Depleting Highway	104.6	35.362	0.26405	0.018508
AUDI	e-tron S	2	496	6500	Charge Depleting UDDS	82.3	50.987	0.26405	0.020894
AUDI	e-tron S	2	496	6500	Charge Depleting Highway	85.3	50.987	0.26405	0.020894
AUDI	e-tron S	3	496	6500	Charge Depleting UDDS	83.6	50.987	0.26405	0.020021
AUDI	e-tron S	3	496	6500	Charge Depleting Highway	87	50.987	0.26405	0.020021
AUDI	e-tron GT	0	523	5500	Charge Depleting UDDS	113.1	40.353	0.41236	0.014608
AUDI	e-tron GT	0	523	5500	Charge Depleting Highway	116.3	40.353	0.41236	0.014608
AUDI	RS e-tron GT	0	637	5500	Charge Depleting UDDS	111.7	40.488	0.48108	0.013793
AUDI	RS e-tron GT	0	637	5500	Charge Depleting Highway	115.3	40.488	0.48108	0.013793
BMW	MINI COOPER SE HARDTOP 2 DOOR	0	181	3500	Charge Depleting UDDS	169.6	27.4	0.431	0.01495
BMW	MINI COOPER SE HARDTOP 2 DOOR	0	181	3500	Charge Depleting Highway	143.5	27.4	0.431	0.01495
BMW	i4 eDrive 40 Gran Coupe (18” Wheels)	0	335	5000	Charge Depleting Highway	154.8	33.9	0.034	0.01668
BMW	i4 eDrive 40 Gran Coupe (18” Wheels)	0	335	5000	Charge Depleting UDDS	156.3	33.9	0.034	0.01668
BMW	i4 eDrive 40 Gran Coupe (19” Wheels)	1	335	5000	Charge Depleting UDDS	145.9	38.2	0.046	0.01715
BMW	i4 eDrive 40 Gran Coupe (19” Wheels)	1	335	5000	Charge Depleting Highway	143.5	38.2	0.046	0.01715
BMW	i4 eDrive 40 Gran Coupe (19” Wheels)	2	335	5000	Charge Depleting UDDS	140.7	42.2	0.057	0.01726
BMW	i4 eDrive 40 Gran Coupe (19” Wheels)	2	335	5000	Charge Depleting Highway	138	42.2	0.057	0.01726
BMW	iX xDrive50 (20” Wheels)	2	516	6000	Charge Depleting UDDS	117.3	43.7	0.175	0.01995
BMW	iX xDrive50 (20” Wheels)	2	516	6000	Charge Depleting Highway	117.7	43.7	0.175	0.01995
BMW	iX xDrive50 (21” Wheels)	0	516	6000	Charge Depleting UDDS	109.4	47.9	0.187	0.02105
BMW	iX xDrive50 (21” Wheels)	0	516	6000	Charge Depleting Highway	111.1	47.9	0.187	0.02105
BMW	iX xDrive50 (21” Wheels)	1	516	6000	Charge Depleting UDDS	115.2	43	0.174	0.02114
BMW	iX xDrive50 (21” Wheels)	1	516	6000	Charge Depleting Highway	116.4	43	0.174	0.02114
BMW	iX xDrive50 (22” Wheels)	3	516	6000	Charge Depleting UDDS	117.1	44	0.175	0.02131

Table A.1 continued from previous page

Make	Model	Vehicle Config #	Rated Power (HP)	ETW (lbs)	Test Procedure Description	FE (MPGe)	A (lbf)	B (lbf/mph)	C (lbf/mph^2)
BMW	iX xDrive50 (22" Wheels)	3	516	6000	Charge Depleting Highway	116.1	44	0.175	0.02131
BMW	i4 M50 Gran Coupe (19" Wheels)	1	536	5250	Charge Depleting UDDS	129	42.8	0.119	0.01635
BMW	i4 M50 Gran Coupe (19" Wheels)	1	536	5250	Charge Depleting Highway	133.8	42.8	0.119	0.01635
BMW	i4 M50 Gran Coupe (19" Wheels)	2	536	5250	Charge Depleting UDDS	122.8	47	0.131	0.01639
BMW	i4 M50 Gran Coupe (19" Wheels)	2	536	5250	Charge Depleting Highway	128.5	47	0.131	0.01639
BMW	i4 M50 Gran Coupe (20" Wheels)	0	536	5250	Charge Depleting UDDS	106.3	59.5	0.167	0.01844
BMW	i4 M50 Gran Coupe (20" Wheels)	0	536	5250	Charge Depleting Highway	107.7	59.5	0.167	0.01844
CHEVROLET	BOLT EUV	1	200	4000	Charge Depleting UDDS	175.4	31.12	0.0175	0.02251
CHEVROLET	BOLT EUV	1	200	4000	Charge Depleting Highway	149.2	31.12	0.0175	0.02251
CHEVROLET	BOLT EUV	1	200	4000	Charge Depleting UDDS	172.9	31.12	0.0175	0.02251
CHEVROLET	BOLT EUV	1	200	4000	Charge Depleting Highway	148.2	31.12	0.0175	0.02251
CHEVROLET	BOLT EUV	2	200	4000	Charge Depleting UDDS	183.5	31.12	0.0175	0.02251
CHEVROLET	BOLT EUV	2	200	4000	Charge Depleting Highway	149.8	31.12	0.0175	0.02251
CHEVROLET	BOLT EV	0	200	3875	Charge Depleting UDDS	129	30.51	0.0152	0.02151
CHEVROLET	BOLT EV	0	200	3875	Charge Depleting Highway	109	30.51	0.0152	0.02151
CHEVROLET	BOLT EV	1	200	3875	Charge Depleting UDDS	132	30.51	0.0152	0.02151
CHEVROLET	BOLT EV	1	200	3875	Charge Depleting Highway	109	30.51	0.0152	0.02151
Ford	Mach-E RWD	0	266	4750	Charge Depleting UDDS	157.4	31.43	0.1279	0.02152
Ford	Mach-E RWD	0	266	4750	Charge Depleting Highway	136.9	31.43	0.1279	0.02152
Ford	Mustang Mach-E AWD	0	266	5000	Charge Depleting UDDS	23.8	33.07	0.2911	0.02106
Ford	Mustang Mach-E AWD	0	266	5000	Charge Depleting Highway	27.4	33.07	0.2911	0.02106
Ford	Mach-E	0	290	5000	Charge Depleting UDDS	146.3	32.69	0.2393	0.02023
Ford	Mach-E	0	290	5000	Charge Depleting Highway	127.3	32.69	0.2393	0.02023
Ford	Mach-E California Route 1	1	290	5000	Charge Depleting Highway	131.8	30.72	0.2336	0.01928
Ford	Mach-E California Route 1	1	290	5000	Charge Depleting UDDS	151.2	30.72	0.2336	0.01928
Ford	Mach-E	0	346	5250	Charge Depleting UDDS	136.2	34.31	0.4009	0.01952
Ford	Mach-E	0	346	5250	Charge Depleting Highway	118.2	34.31	0.4009	0.01952
Ford	Mach-E Extended Range AWD	0	346	5000	Charge Depleting UDDS	149.3	30.71	0.2874	0.02015
Ford	Mach-E Extended Range AWD	0	346	5000	Charge Depleting Highway	130.5	30.71	0.2874	0.02015
Ford	Mach-E GT Base	0	480	5250	Charge Depleting UDDS	26.2	38.74	0.344	0.02118
Ford	Mach-E GT Base	0	480	5250	Charge Depleting Highway	30.5	38.74	0.344	0.02118
Ford	Mach-E GT Performance Edition	0	480	5250	Charge Depleting UDDS	125.8	44.66	0.3522	0.02144
Ford	Mach-E GT Performance Edition	0	480	5250	Charge Depleting Highway	107.6	44.66	0.3522	0.02144
HYUNDAI	Kona Electric	0	37	4000	Charge Depleting UDDS	17.2	24.859	-0.20036	0.023656
HYUNDAI	Kona Electric	0	37	4000	Charge Depleting Highway	21.7	24.859	-0.20036	0.023656
Hyundai	Ioniq 5	0	167	4250	Charge Depleting UDDS	18.3	18.868	0.59641	0.016432

Table A.1 continued from previous page

Make	Model	Vehicle Config #	Rated Power (HP)	ETW (lbs)	Test Procedure Description	FE (MPGe)	A (lbf)	B (lbf/mph)	C (lbf/mph^2)
Hyundai	Ioniq 5	0	167	4250	Charge Depleting Highway	24.7	18.868	0.59641	0.016432
Hyundai	Ioniq 5	0	225	4500	Charge Depleting UDDS	17.6	25.158	0.10857	0.022881
Hyundai	Ioniq 5	0	225	4500	Charge Depleting Highway	23.9	25.158	0.10857	0.022881
Hyundai	Ioniq 5	0	320	5000	Charge Depleting UDDS	22.4	34.342	0.21928	0.022718
Hyundai	Ioniq 5	0	320	5000	Charge Depleting Highway	27.4	34.342	0.21928	0.022718
Hyundai	Ioniq 5	1	320	4750	Charge Depleting UDDS	21.1	26.849	0.40922	0.020726
Hyundai	Ioniq 5	1	320	4750	Charge Depleting Highway	26.9	26.849	0.40922	0.020726
Hyundai	Ioniq 5	1	320	4750	Charge Depleting UDDS	21.4	26.849	0.40922	0.020726
Hyundai	Ioniq 5	1	320	4750	Charge Depleting Highway	27.1	26.849	0.40922	0.020726
Jaguar	I-Pace EV400	0	400	5250	Charge Depleting UDDS	103.8	48.599	0.64016	0.01862
Jaguar	I-Pace EV400	0	400	5250	Charge Depleting Highway	97.9	48.599	0.64016	0.01862
Jaguar	I-Pace EV400 (Autonomous)	0	400	5250	Charge Depleting UDDS	119.9	34.178	0.75123	0.017701
Jaguar	I-Pace EV400 (Autonomous)	0	400	5250	Charge Depleting Highway	106.9	34.178	0.75123	0.017701
Jaguar	I-PACE SE	1	400	5250	Charge Depleting UDDS	111	38.881	0.64016	0.018981
Jaguar	I-PACE SE	1	400	5250	Charge Depleting Highway	101.9	38.881	0.64016	0.018981
Kia	Niro Electric	0	38	4250	Charge Depleting UDDS	19.2	32.717	-0.1911	0.023073
Kia	Niro Electric	0	38	4250	Charge Depleting Highway	23.3	32.717	-0.1911	0.023073
KIA	EV6	0	167	4250	Charge Depleting UDDS	17.1	23.365	0.16194	0.021063
KIA	EV6	0	167	4250	Charge Depleting Highway	23.2	23.365	0.16194	0.021063
KIA	EV6	0	225	4500	Charge Depleting UDDS	17.1	23.313	0.11939	0.022206
KIA	EV6	0	225	4500	Charge Depleting Highway	22.7	23.313	0.11939	0.022206
KIA	EV6	0	320	4750	Charge Depleting UDDS	20.8	33.661	0.14685	0.022228
KIA	EV6	0	320	4750	Charge Depleting Highway	26.2	33.661	0.14685	0.022228
KIA	EV6	1	320	4750	Charge Depleting UDDS	19.7	23.992	0.2289	0.020912
KIA	EV6	1	320	4750	Charge Depleting Highway	24.2	23.992	0.2289	0.020912
Lucid	Air Grand Touring	0	819	5500	Charge Depleting UDDS	173.6	32.398	0.151	0.012
Lucid	Air Grand Touring	0	819	5500	Charge Depleting Highway	176.4	32.398	0.151	0.012
Lucid	Air Grand Touring	1	819	5500	Charge Depleting UDDS	149.3	39.36	0.1315	0.01261
Lucid	Air Grand Touring	1	819	5500	Charge Depleting Highway	151.2	39.36	0.1315	0.01261
Lucid	Air Dream R	0	933	5500	Charge Depleting Highway	167.1	32.372	0.153	0.012
Lucid	Air Dream R	0	933	5500	Charge Depleting UDDS	167.4	32.372	0.153	0.012
Lucid	Air Dream R	1	933	5500	Charge Depleting UDDS	153.1	39.35	0.1319	0.0126
Lucid	Air Dream R	1	933	5500	Charge Depleting Highway	155.4	39.35	0.1319	0.0126
Lucid	Air Dream P	0	1111	5500	Charge Depleting UDDS	155.4	34.19	0.1331	0.01444
Lucid	Air Dream P	0	1111	5500	Charge Depleting Highway	152.6	34.19	0.1331	0.01444
Lucid	Air Dream P	1	1111	5500	Charge Depleting UDDS	146.9	39.49	0.2081	0.01247

Table A.1 continued from previous page

Make	Model	Vehicle Config #	Rated Power (HP)	ETW (lbs)	Test Procedure Description	FE (MPGe)	A (lbf)	B (lbf/mph)	C (lbf/mph^2)
Lucid	Air Dream P	1	1111	5500	Charge Depleting Highway	148.4	39.49	0.2081	0.01247
MAZDA	MX-30	0	108	4000	Charge Depleting UDDS	140.1	29.97	0.38976	0.020128
MAZDA	MX-30	0	108	4000	Charge Depleting Highway	121.4	29.97	0.38976	0.020128
Mercedes-Benz	EQS 450+	0	329	6000	Charge Depleting UDDS	138	41.81	0.4521	0.0117
Mercedes-Benz	EQS 450+	0	329	6000	Charge Depleting Highway	38.1	41.81	0.4521	0.0117
Mercedes-Benz	AMG EQS 4MATIC+	0	516	6500	Charge Depleting UDDS	108.2	55.08	0.7234	0.0117
Mercedes-Benz	AMG EQS 4MATIC+	0	516	6500	Charge Depleting Highway	111.1	55.08	0.7234	0.0117
Mercedes-Benz	EQS 580 4MATIC	0	516	6000	Charge Depleting UDDS	124.5	48.56	0.4521	0.0117
Mercedes-Benz	EQS 580 4MATIC	0	516	6000	Charge Depleting Highway	134.4	48.56	0.4521	0.0117
NISSAN	LEAF	0	147	3875	Charge Depleting Highway	141.1	25.89	0.3449	0.01945
NISSAN	LEAF	0	147	3875	Charge Depleting UDDS	174	25.89	0.3449	0.01945
NISSAN	LEAF	1	147	3875	Charge Depleting UDDS	177.1	25.89	0.3449	0.01945
NISSAN	LEAF	1	147	3875	Charge Depleting Highway	141.3	25.89	0.3449	0.01945
NISSAN	LEAF	4	214	4250	Charge Depleting UDDS	167.8	28.15	0.2892	0.02009
NISSAN	LEAF	4	214	4250	Charge Depleting Highway	138.9	28.15	0.2892	0.02009
NISSAN	LEAF	5	214	4250	Charge Depleting UDDS	169.1	28.15	0.2892	0.02009
NISSAN	LEAF	5	214	4250	Charge Depleting Highway	139.1	28.15	0.2892	0.02009
NISSAN	LEAF SV/SL	0	214	4250	Charge Depleting UDDS	162.6	30.36	0.3201	0.01956
NISSAN	LEAF SV/SL	0	214	4250	Charge Depleting Highway	133.3	30.36	0.3201	0.01956
NISSAN	LEAF SV/SL	1	214	4250	Charge Depleting UDDS	164.5	30.36	0.3201	0.01956
NISSAN	LEAF SV/SL	1	214	4250	Charge Depleting Highway	136.1	30.36	0.3201	0.01956
Polestar	Polestar2 Single Motor	0	228	4750	Charge Depleting UDDS	159.5	31.11	0.2191	0.01625
Polestar	Polestar2 Single Motor	0	228	4750	Charge Depleting Highway	141.3	31.11	0.2191	0.01625
Polestar2 Dual Motor	Polestar2 Dual Motor	0	402	5000	Charge Depleting UDDS	130.1	34.52	0.2109	0.01648
Polestar2 Dual Motor	Polestar2 Dual Motor	0	402	5000	Charge Depleting Highway	116.9	34.52	0.2109	0.01648
Porsche	Taycan Perf Battery	0	321	5000	Charge Depleting UDDS	112.8	38.51	0.43415	0.01304
Porsche	Taycan Perf Battery	0	321	5000	Charge Depleting Highway	124.4	38.51	0.43415	0.01304
Porsche	Taycan 4 Cross Turismo	0	375	5500	Charge Depleting UDDS	108.7	41.904	0.483	0.015546
Porsche	Taycan 4 Cross Turismo	0	375	5500	Charge Depleting Highway	109.8	41.904	0.483	0.015546
Porsche	Taycan Perf Battery Plus	0	375	5250	Charge Depleting UDDS	101.9	38.51	0.43415	0.01304
Porsche	Taycan Perf Battery Plus	0	375	5250	Charge Depleting Highway	114.3	38.51	0.43415	0.01304
Porsche	Taycan 4S Perf Battery	0	429	5250	Charge Depleting UDDS	112.5	41.972	0.43415	0.012053
Porsche	Taycan 4S Perf Battery	0	429	5250	Charge Depleting Highway	112.5	41.972	0.43415	0.012053
Porsche	Taycan 4S Cross Turismo	0	482	5500	Charge Depleting UDDS	108	41.904	0.483	0.015546
Porsche	Taycan 4S Cross Turismo	0	482	5500	Charge Depleting Highway	108.6	41.904	0.483	0.015546
Porsche	Taycan 4S Perf Battery Plus	0	482	5500	Charge Depleting UDDS	106.8	43.478	0.43415	0.012053

Table A.1 continued from previous page

Make	Model	Vehicle Config #	Rated Power (HP)	ETW (lbs)	Test Procedure Description	FE (MPGe)	A (lbf)	B (lbf/mph)	C (lbf/mph^2)
Porsche	Taycan 4S Perf Battery Plus	0	482	5500	Charge Depleting Highway	115.9	43.478	0.43415	0.012053
Porsche	Taycan Turbo	0	616	5500	Charge Depleting UDDS	105.3	47.48	0.43415	0.013392
Porsche	Taycan Turbo	0	616	5500	Charge Depleting Highway	111.2	47.48	0.43415	0.013392
Porsche	Taycan Turbo	0	616	5500	Charge Depleting UDDS	99	51.279	0.43415	0.014673
Porsche	Taycan Turbo	0	616	5500	Charge Depleting Highway	101.5	51.279	0.43415	0.014673
Porsche	Taycan Turbo Cross Turismo	0	616	5500	Charge Depleting UDDS	102.8	47.525	0.53473	0.014847
Porsche	Taycan Turbo Cross Turismo	0	616	5500	Charge Depleting Highway	102.6	47.525	0.53473	0.014847
Porsche	Taycan Turbo S Cross Turismo	0	616	5500	Charge Depleting UDDS	105	43.006	0.4924	0.017933
Porsche	Taycan Turbo S Cross Turismo	0	616	5500	Charge Depleting Highway	104.1	43.006	0.4924	0.017933
Rivian	R1S	0	872	7000	Charge Depleting Highway	33.2	44.5	0.689	0.0199
Rivian	R1S	0	872	7000	Charge Depleting UDDS	29.8	44.5	0.689	0.0199
Rivian	R1S	1	872	7000	Charge Depleting Highway	37.9	49.975	0.36541	0.023407
Rivian	R1S	1	872	7000	Charge Depleting UDDS	33.9	49.975	0.36541	0.023407
Rivian	R1T	2	872	7000	Charge Depleting Highway	34.5	44.81	0.9309	0.01765
Rivian	R1T	2	872	7000	Charge Depleting UDDS	30.4	44.81	0.9309	0.01765
Rivian	R1T	3	872	7000	Charge Depleting Highway	33.9	48.47	0.7674	0.01799
Rivian	R1T	3	872	7000	Charge Depleting UDDS	29.4	48.47	0.7674	0.01799
Tesla	Model 3 RWD	0	257	4250	Charge Depleting UDDS	185.3	37.17	0.047	0.0144
Tesla	Model 3 RWD	0	257	4250	Charge Depleting Highway	170.1	37.17	0.047	0.0144
Tesla	Model Y Standard Range RWD	0	280	4250	Charge Depleting UDDS	190.8	25.02	0.4847	0.0121
Tesla	Model Y Standard Range RWD	0	280	4250	Charge Depleting Highway	162	25.02	0.4847	0.0121
Tesla	Model Y AWD	0	390	4750	Charge Depleting UDDS	167.3	34.26	0.3191	0.0142
Tesla	Model Y AWD	0	390	4750	Charge Depleting Highway	150.9	34.26	0.3191	0.0142
Tesla	Model Y Long Range AWD	0	390	4750	Charge Depleting UDDS	164.8	34.26	0.3191	0.0142
Tesla	Model Y Long Range AWD	0	390	4750	Charge Depleting Highway	152.1	34.26	0.3191	0.0142
Tesla	Model 3 Long Range AWD	0	393	4250	Charge Depleting UDDS	184.5	34.98	0.0865	0.0148
Tesla	Model 3 Long Range AWD	0	393	4250	Charge Depleting Highway	173.4	34.98	0.0865	0.0148
Tesla	Model Y Performance AWD	0	418	4750	Charge Depleting Highway	137.5	45.49	0.172	0.016
Tesla	Model Y Performance AWD	0	418	4750	Charge Depleting UDDS	149.6	45.49	0.172	0.016
Tesla	Model 3 Performance AWD	0	430	4250	Charge Depleting UDDS	157.3	49.01	-0.2001	0.02
Tesla	Model 3 Performance AWD	0	430	4250	Charge Depleting Highway	143.1	49.01	-0.2001	0.02
Tesla	Model X Long Range	0	658	5500	Charge Depleting UDDS	144.7	33.56	0.4237	0.0168
Tesla	Model X Long Range	0	658	5500	Charge Depleting Highway	131.3	33.56	0.4237	0.0168
Tesla	Model S Long Range	0	662	4750	Charge Depleting UDDS	163.9	28.99	0.4592	0.0111
Tesla	Model S Long Range	0	662	4750	Charge Depleting Highway	151.3	28.99	0.4592	0.0111
Tesla	Model X Plaid (20” Wheels)	1	925	5500	Charge Depleting UDDS	138.6	30.62	0.7106	0.0136

Table A.1 continued from previous page

Make	Model	Vehicle Config #	Rated Power (HP)	ETW (lbs)	Test Procedure Description	FE (MPGe)	A (lbf)	B (lbf/mph)	C (lbf/mph^2)
Tesla	Model X Plaid (20" Wheels)	1	925	5500	Charge Depleting Highway	125.7	30.62	0.7106	0.0136
Tesla	Model X Plaid (22" Wheels)	0	925	5500	Charge Depleting UDDS	127	43.5	0.5119	0.0155
Tesla	Model X Plaid (22" Wheels)	0	925	5500	Charge Depleting Highway	119.1	43.5	0.5119	0.0155
Tesla	Model S Plaid (19" Wheels)	0	1006	5000	Charge Depleting UDDS	154.5	29.64	0.6164	0.01
Tesla	Model S Plaid (19" Wheels)	0	1006	5000	Charge Depleting Highway	145.2	29.64	0.6164	0.01
Tesla	Model S Plaid (21" Wheels)	0	1006	5000	Charge Depleting UDDS	133.1	43.3	0.5143	0.0109
Tesla	Model S Plaid (21" Wheels)	0	1006	5000	Charge Depleting Highway	128.3	43.3	0.5143	0.0109
Volkswagen	ID.4 Pro	0	201	4750	Charge Depleting UDDS	168.2	23.987	0.29124	0.016006
Volkswagen	ID.4 Pro	0	201	4750	Charge Depleting Highway	142.7	23.987	0.29124	0.016006
Volkswagen	ID.4 Pro	0	201	4750	Charge Depleting UDDS	170.9	23.987	0.29124	0.016006
Volkswagen	ID.4 Pro	0	201	4750	Charge Depleting Highway	142.8	23.987	0.29124	0.016006
Volkswagen	ID.4 Pro S	1	201	5000	Charge Depleting UDDS	159.4	27.966	0.29124	0.016495
Volkswagen	ID.4 Pro S	1	201	5000	Charge Depleting Highway	136.3	27.966	0.29124	0.016495
Volkswagen	ID.4 Pro S	1	201	5000	Charge Depleting UDDS	160.9	27.966	0.29124	0.016495
Volkswagen	ID.4 Pro S	1	201	5000	Charge Depleting Highway	135.4	27.966	0.29124	0.016495
Volkswagen	ID.4 AWD Pro	0	295	5000	Charge Depleting Highway	137.4	25.136	0.38734	0.015971
Volkswagen	ID.4 AWD Pro	0	295	5000	Charge Depleting UDDS	147.9	25.136	0.38734	0.015971
Volkswagen	ID.4 AWD Pro	0	295	5000	Charge Depleting UDDS	153.8	25.136	0.38734	0.015971
Volkswagen	ID.4 AWD Pro	0	295	5000	Charge Depleting Highway	136.9	25.136	0.38734	0.015971
Volkswagen	ID.4 AWD Pro S	1	295	5250	Charge Depleting UDDS	139.3	28.76	0.38734	0.016821
Volkswagen	ID.4 AWD Pro S	1	295	5250	Charge Depleting Highway	129.2	28.76	0.38734	0.016821
Volkswagen	ID.4 AWD Pro S	1	295	5250	Charge Depleting UDDS	145.1	28.76	0.38734	0.016821
Volkswagen	ID.4 AWD Pro S	1	295	5250	Charge Depleting Highway	128.2	28.76	0.38734	0.016821
Volvo	C40 Recharge twin	0	402	5000	Charge Depleting UDDS	132	30.9	0.4793	0.01934
Volvo	C40 Recharge twin	0	402	5000	Charge Depleting Highway	112.4	30.9	0.4793	0.01934
Volvo	XC40 Recharge twin	0	402	5000	Charge Depleting UDDS	128.4	30.9	0.4793	0.02025
Volvo	XC40 Recharge twin	0	402	5000	Charge Depleting Highway	109.9	30.9	0.4793	0.02025

Appendix B

EPA Chosen Vehicle Data

The following table includes the list of BEVs chosen for analysis from Appendix A. The documents used for finding this information is found in the Application for Certification documents uploaded to the EPA Transportation and Air Quality Document Index System, which also contain the Certificate Summary Information Report [5]. Document ID numbers are provided in the following table for reference.

Table B.1: List of chosen vehicles and parameters taken from 2022 EPA CSI data

Doc ID	Vehicle	Cycle	Weight (lbs)	DC Discharge Energy (kWh)	AC Recharge Energy (kWh)	Range (mi)	MFG FE (MPGe)	Charge Eff.	A	B	C	Rated Power (HP)
53765	Rivian R1S Conserve	HWY	7000	129	152	450	100	85%	44.5	0.689	0.020	436
53765	Rivian R1S Conserve	UDDS	7000	129	152	503	112	85%	44.5	0.689	0.020	436
53765	Rivian R1S Sport	HWY	7000	129	153	397	88	84%	50.0	0.365	0.023	872
53765	Rivian R1S Sport	UDDS	7000	129	153	444	98	84%	50.0	0.365	0.023	872
53763	Rivian R1T Conserve	HWY	7000	129	153	431	95	86%	44.8	0.931	0.018	436
53763	Rivian R1T Conserve	UDDS	7000	129	153	491	108	86%	44.8	0.931	0.018	436
53765	Rivian R1T Conserve	US06	7000	129	153	8.01	83	86%	44.8	0.931	0.018	436
53763	Rivian R1T Sport	HWY	7000	129	147	381	87	88%	48.5	0.767	0.018	872
53763	Rivian R1T Sport	UDDS	7000	129	147	429	99	88%	48.5	0.767	0.018	872
53765	Rivian R1T Sport	US06	7000	129	147	8.01	80	88%	48.5	0.767	0.018	872
52673	Chevrolet Bolt EV Config 1	UDDS	3875	66	74	397	182	90%	28.4	0.202	0.019	200
52673	Chevrolet Bolt EV Config 1	HWY	3875	66	74	336	154	90%	28.4	0.202	0.019	200
52673	Chevrolet Bolt EV Config 2	UDDS	3875	66	74	397	182	90%	28.4	0.202	0.019	200
52673	Chevrolet Bolt EV Config 2	HWY	3875	66	74	336	154	90%	28.4	0.202	0.019	200
54826	Ford Mustang Mach-E AWD	UDDS	4750	68	78	295	128	87%	43.7	0.246	0.021	266
54826	Ford Mustang Mach-E AWD	HWY	4750	68	78	262	114	87%	43.7	0.246	0.021	266
54828	Ford Mustang Mach-E RWD	UDDS	4750	68	78	335	145	87%	35.9	0.167	0.021	266
54828	Ford Mustang Mach-E RWD	HWY	4750	68	78	292	127	87%	35.9	0.167	0.021	266
54516	Ford Mustang Mach-E AWD ER	UDDS	5250	88	101	372	124	87%	46.8	0.260	0.021	346
54516	Ford Mustang Mach-E AWD ER	HWY	5250	88	101	339	113	87%	46.8	0.260	0.021	346
54517	Ford Mustang Mach-E RWD ER	UDDS	5000	89	102	435	145	87%	37.9	0.174	0.021	290
54517	Ford Mustang Mach-E RWD ER	HWY	5000	89	102	383	127	87%	37.9	0.174	0.021	290
54971	Tesla Model Y AWD P	UDDS	4750	81	92	409	150	88%	45.5	0.172	0.016	418
54971	Tesla Model Y AWD P	HWY	4750	81	92	376	138	88%	45.5	0.172	0.016	418

Table B.1 continued from previous page

Doc ID	Vehicle	Cycle	Weight (lbs)	DC Discharge Energy (kWh)	AC Recharge Energy (kWh)	Range (mi)	MFG FE (MPGe)	Charge Eff.	A	B	C	Rated Power (HP)
54971	Tesla Model Y AWD P	US06	4750	81	92	8.01	115	88%	45.5	0.172	0.016	418
54971	Tesla Model Y AWD LR	UDDS	4750	81	91	446	165	89%	34.3	0.319	0.014	390
54971	Tesla Model Y AWD LR	HWY	4750	81	91	411	152	89%	34.3	0.319	0.014	390
54289	Tesla Model Y RWD	UDDS	4250	55	63	357	191	87%	25.0	0.485	0.012	280
54289	Tesla Model Y RWD	HWY	4250	55	63	303	162	87%	25.0	0.485	0.012	280
54288	Tesla Model 3 RWD	UDDS	4250	62	70	383	185	89%	37.2	0.047	0.014	257
54288	Tesla Model 3 RWD	HWY	4250	62	70	351	170	89%	37.2	0.047	0.014	257
54290	Tesla Model 3 AWD P	UDDS	4250	81	94	440	157	86%	49.0	-0.200	0.020	430
54290	Tesla Model 3 AWD P	HWY	4250	81	94	400	143	86%	49.0	-0.200	0.020	430
54290	Tesla Model 3 AWD P	US06	4250	81	94	8.01	128	86%	49.0	-0.200	0.020	430
54290	Tesla Model 3 AWD LR	UDDS	4250	82	92	505	184	89%	35.0	0.087	0.015	393
54290	Tesla Model 3 AWD LR	HWY	4250	82	92	475	173	89%	35.0	0.087	0.015	393
54290	Tesla Model 3 AWD LR	US06	4250	82	92	8.01	139	89%	35.0	0.087	0.015	393
54521	Kia EV6 AWD LR 20 in	UDDS	4750	77	87	419	162	89%	33.7	0.147	0.022	320
54521	Kia EV6 AWD LR 20 in	HWY	4750	77	87	333	129	89%	33.7	0.147	0.022	320
54521	Kia EV6 AWD LR 19 in	UDDS	4750	77	87	439	171	89%	24.0	0.229	0.021	320
54521	Kia EV6 AWD LR 19 in	HWY	4750	77	87	358	139	89%	24.0	0.229	0.021	320
54524	Kia EV6 RWD LR	UDDS	4500	77	86	505	197	90%	23.3	0.119	0.022	225
54524	Kia EV6 RWD LR	HWY	4500	77	86	379	148	90%	23.3	0.119	0.022	225
52872	Nissan Leaf SV/SL FWD	UDDS	4250	60	68	330	163	87%	30.4	0.320	0.020	214
52872	Nissan Leaf SV/SL FWD	HWY	4250	60	68	270	133	87%	30.4	0.320	0.020	214
52871	Nissan Leaf FWD	UDDS	3875	39	45	231	174	88%	25.9	0.345	0.019	147
52871	Nissan Leaf FWD	HWY	3875	39	45	188	141	88%	25.9	0.345	0.019	147
55142	Lucid Air Dream P 21 in	UDDS	5500	118	137	598	147	86%	39.5	0.208	0.012	1111

Table B.1 continued from previous page

Doc ID	Vehicle	Cycle	Weight (lbs)	DC Discharge Energy (kWh)	AC Recharge Energy (kWh)	Range (mi)	MFG FE (MPGe)	Charge Eff.	A	B	C	Rated Power (HP)
55142	Lucid Air Dream P 21 in	HWY	5500	118	137	604	148	86%	39.5	0.208	0.012	1111
55142	Lucid Air Dream P 21 in	US06	5500	89	112	8	113	79%	39.5	0.208	0.012	1111
52492	Hyundai Kona Electric	UDDS	4000	64	71	414	196	90%	24.9	-0.200	0.024	201
52492	Hyundai Kona Electric	HWY	4000	64	71	329	156	90%	24.9	-0.200	0.024	201
52996	Audi e-tron S	UDDS	6500	87	97	280	98	90%	35.4	0.264	0.020	496
52996	Audi e-tron S	HWY	6500	87	97	289	101	90%	35.4	0.264	0.020	496
53895	Mercedes EQS 450+	UDDS	6000	111	122	498	138	91%	41.8	0.452	0.012	329
53895	Mercedes EQS 450+	HWY	6000	111	122	499	138	91%	41.8	0.452	0.012	329
53895	Mercedes EQS 450+	US06	6000	111	122	8	107	91%	41.8	0.452	0.012	329
54998	Porsche Taycan 4S Perf Battery	UDDS	5250	71	90	301	113	79%	42.0	0.434	0.012	375
54998	Porsche Taycan 4S Perf Battery	HWY	5250	71	90	307	113	79%	42.0	0.434	0.012	375

Appendix C

US06 Energy Consumption Data

The following table includes the list of vehicles with available US06 energy consumption data found in the submitted CSI documents [5]. Specific documents numbers used for this information can be found in Appendix B.

Table C.1: List of chosen vehicles with US06 energy consumption data available

Make	**Model**	**FE (kWh/100 mi)**	**FE (MPGe)**
Rivian	R1T Conserve	40.8	82.7
Rivian	R1T Sport	42.2	79.9
Tesla	Model Y AWD P	29.3	114.9
Tesla	Model 3 AWD P	26.2	128.5
Tesla	Model 3 AWD LR	24.2	139.2
Lucid	Air Dream P 21 in	29.7	113.4
Mercedes	EQS 450+	31.6	106.6

Appendix D

Additional Results for Base Model

Table D.1: Percentage error for predicting the HWFET power consumption using the base model and fitted UDDS/HWFET data.

Vehicle	**Estimated** $\mathbf{P^{net}_{batt}}$ **[kW]**	**Actual** $\mathbf{P^{net}_{batt}}$ **[kW]**	**% Error**
Rivian R1S Conserve	14.52	5.01	5.0%
Rivian R1S Sport	14.34	5.69	-8.5%
Rivian R1T Conserve	15.20	5.23	3.6%
Rivian R1T Sport	14.82	5.87	-9.1%
Chevrolet Bolt EV, Config 1	10.24	3.26	7.9%
Chevrolet Bolt EV, Config 2	10.24	3.26	8.0%
Ford Mustang Mach-E AWD	12.45	4.49	-0.1%
Ford Mustang Mach-E RWD	11.38	3.97	1.5%
Ford Mustang Mach-E AWD ER	12.81	4.67	1.6%
Ford Mustang Mach-E RWD ER	11.55	4.00	3.2%
Tesla Model Y AWD P	10.95	3.88	5.3%
Tesla Model Y AWD LR	10.09	3.55	6.5%
Tesla Model Y RWD	9.45	3.01	8.3%
Tesla Model 3 RWD	9.05	3.18	6.1%
Tesla Model 3 AWD P	10.46	3.60	7.3%
Tesla Model 3 AWD LR	9.14	3.18	9.4%
Kia EV6 AWD LR 20 in	11.26	3.62	0.2%
Kia EV6 AWD LR 19 in	10.35	3.46	-0.9%
Kia EV6 RWD LR	10.06	3.00	2.1%
Nissan Leaf SV/SL FWD	11.11	3.55	4.1%
Nissan Leaf FWD	10.75	3.33	6.6%
Lucid Air Dream P 21 in	9.60	3.86	1.9%
Hyundai Kona Electric	8.97	3.04	-4.8%
Audi e-tron S	11.39	6.06	-21.3%
Mercedes EQS 450+	10.88	4.38	1.0%
Porsche Taycan 4S Perf Battery	10.90	4.62	-4.3%

Appendix E

Additional Results for Model Normalized by Weight

Table E.1: Percentage error for estimating the HWFET power consumption using the model normalized by test weight.

Vehicle	**Estimated** $\mathbf{P^{net}_{batt}}$ **[kW]**	**Actual** $\mathbf{P^{net}_{batt}}$ **[kW]**	**% Error**
Rivian R1S Conserve	14.81	5.01	7.1%
Rivian R1S Sport	14.64	5.69	-6.6%
Rivian R1T Conserve	15.46	5.23	5.5%
Rivian R1T Sport	15.10	5.87	-7.4%
Chevrolet Bolt EV, Config 1	9.79	3.26	3.1%
Chevrolet Bolt EV, Config 2	9.79	3.26	3.2%
Ford Mustang Mach-E AWD	12.17	4.49	-2.4%
Ford Mustang Mach-E RWD	11.14	3.97	-0.7%
Ford Mustang Mach-E AWD ER	12.66	4.67	0.4%
Ford Mustang Mach-E RWD ER	11.37	4.00	1.6%
Tesla Model Y AWD P	10.72	3.88	3.1%
Tesla Model Y AWD LR	9.89	3.55	4.4%
Tesla Model Y RWD	9.13	3.01	4.6%
Tesla Model 3 RWD	8.74	3.18	2.5%
Tesla Model 3 AWD P	10.10	3.60	3.6%
Tesla Model 3 AWD LR	8.82	3.18	5.7%
Kia EV6 AWD LR 20 in	11.02	3.62	-1.9%
Kia EV6 AWD LR 19 in	10.14	3.46	-2.9%
Kia EV6 RWD LR	9.79	3.00	-0.7%
Nissan Leaf SV/SL FWD	10.73	3.55	0.6%
Nissan Leaf FWD	10.28	3.33	1.9%
Lucid Air Dream P 21 in	9.63	3.86	2.2%
Hyundai Kona Electric	8.59	3.04	-8.8%
Audi e-tron S	11.64	6.06	-19.5%
Mercedes EQS 450+	11.01	4.38	2.2%
Porsche Taycan 4S Perf Battery	10.81	4.62	-5.1%

Appendix F

Additional Results for Model Normalized by Performance

Table F.1: Percentage error for predicting the UDDS power consumption using the model normalized by performance.

Vehicle	**Estimated** $\mathbf{P^{net}_{batt}}$ **[kW]**	**Actual** $\mathbf{P^{net}_{batt}}$ **[kW]**	**% Error**
Rivian R1S Conserve	4.74	5.01	-5.4%
Rivian R1S Sport	5.88	5.69	3.2%
Rivian R1T Conserve	4.96	5.23	-5.3%
Rivian R1T Sport	6.08	5.87	3.5%
Chevrolet Bolt EV, Config 1	3.25	3.26	-0.5%
Chevrolet Bolt EV, Config 2	3.25	3.26	-0.4%
Ford Mustang Mach-E AWD	4.08	4.49	-9.1%
Ford Mustang Mach-E RWD	3.69	3.97	-7.1%
Ford Mustang Mach-E AWD ER	4.41	4.67	-5.6%
Ford Mustang Mach-E RWD ER	3.80	4.00	-4.9%
Tesla Model Y AWD P	4.44	3.88	14.4%
Tesla Model Y AWD LR	3.97	3.55	11.9%
Tesla Model Y RWD	3.40	3.01	13.1%
Tesla Model 3 RWD	3.36	3.18	5.6%
Tesla Model 3 AWD P	4.54	3.60	26.1%
Tesla Model 3 AWD LR	3.93	3.18	23.4%
Kia EV6 AWD LR 20 in	3.82	3.62	5.5%
Kia EV6 AWD LR 19 in	3.46	3.46	0.2%
Kia EV6 RWD LR	3.03	3.00	1.0%
Nissan Leaf SV/SL FWD	3.46	3.55	-2.4%
Nissan Leaf FWD	3.07	3.33	-7.7%
Lucid Air Dream P 21 in	6.20	3.86	60.5%
Hyundai Kona Electric	2.77	3.04	-9.0%
Audi e-tron S	4.09	6.06	-32.5%
Mercedes EQS 450+	3.83	4.38	-12.6%
Porsche Taycan 4S Perf Battery	4.14	4.62	-10.5%

Table F.2: Percentage error for predicting the HWFET power consumption using the model normalized by performance and fitted UDDS/HWFET data.

Vehicle	**Estimated** $\mathbf{P^{net}_{batt}}$ **[kW]**	**Actual** $\mathbf{P^{net}_{batt}}$ **[kW]**	**% Error**
Rivian R1S Conserve	14.36	5.01	3.9%
Rivian R1S Sport	15.34	5.69	-2.1%
Rivian R1T Conserve	15.03	5.23	2.5%
Rivian R1T Sport	15.82	5.87	-3.0%
Chevrolet Bolt EV, Config 1	9.90	3.26	4.3%
Chevrolet Bolt EV, Config 2	9.90	3.26	4.4%
Ford Mustang Mach-E AWD	12.18	4.49	-2.3%
Ford Mustang Mach-E RWD	11.12	3.97	-0.8%
Ford Mustang Mach-E AWD ER	12.73	4.67	0.9%
Ford Mustang Mach-E RWD ER	11.32	4.00	1.2%
Tesla Model Y AWD P	11.29	3.88	8.6%
Tesla Model Y AWD LR	10.32	3.55	8.9%
Tesla Model Y RWD	9.38	3.01	7.5%
Tesla Model 3 RWD	8.88	3.18	4.1%
Tesla Model 3 AWD P	11.04	3.60	13.3%
Tesla Model 3 AWD LR	9.56	3.18	14.5%
Kia EV6 AWD LR 20 in	11.21	3.62	-0.2%
Kia EV6 AWD LR 19 in	10.31	3.46	-1.4%
Kia EV6 RWD LR	9.70	3.00	-1.7%
Nissan Leaf SV/SL FWD	10.74	3.55	0.7%
Nissan Leaf FWD	10.16	3.33	0.7%
Lucid Air Dream P 21 in	12.07	3.86	28.0%
Hyundai Kona Electric	8.61	3.04	-8.6%
Audi e-tron S	11.50	6.06	-20.5%
Mercedes EQS 450+	10.60	4.38	-1.6%
Porsche Taycan 4S Perf Battery	10.93	4.62	-4.1%

Appendix G

Additional Results for Model Normalized by Weight/Performance

Table G.1: Percentage error for estimating the UDDS power consumption using the model normalized by weight and performance.

Vehicle	**Estimated** $\mathbf{P^{net}_{batt}}$ **[kW]**	**Actual** $\mathbf{P^{net}_{batt}}$ **[kW]**	**% Error**
Rivian R1S Conserve	5.17	5.01	3.0%
Rivian R1S Sport	6.70	5.69	17.7%
Rivian R1T Conserve	5.38	5.23	2.9%
Rivian R1T Sport	6.90	5.87	17.5%
Chevrolet Bolt EV, Config 1	3.02	3.26	-7.5%
Chevrolet Bolt EV, Config 2	3.02	3.26	-7.4%
Ford Mustang Mach-E AWD	4.02	4.49	-10.6%
Ford Mustang Mach-E RWD	3.62	3.97	-8.9%
Ford Mustang Mach-E AWD ER	4.44	4.67	-4.9%
Ford Mustang Mach-E RWD ER	3.78	4.00	-5.5%
Tesla Model Y AWD P	4.31	3.88	11.2%
Tesla Model Y AWD LR	3.85	3.55	8.6%
Tesla Model Y RWD	3.19	3.01	6.2%
Tesla Model 3 RWD	3.16	3.18	-0.4%
Tesla Model 3 AWD P	4.21	3.60	17.0%
Tesla Model 3 AWD LR	3.63	3.18	13.9%
Kia EV6 AWD LR 20 in	3.73	3.62	2.9%
Kia EV6 AWD LR 19 in	3.37	3.46	-2.5%
Kia EV6 RWD LR	2.92	3.00	-2.7%
Nissan Leaf SV/SL FWD	3.31	3.55	-6.7%
Nissan Leaf FWD	2.91	3.33	-12.6%
Lucid Air Dream P 21 in	6.42	3.86	66.2%
Hyundai Kona Electric	2.56	3.04	-15.7%
Audi e-tron S	4.46	6.06	-26.4%
Mercedes EQS 450+	4.00	4.38	-8.6%
Porsche Taycan 4S Perf Battery	4.17	4.62	-9.9%

Table G.2: Percentage error for estimating the HWFET power consumption using the model normalized by test weight and performance.

Vehicle	**Estimated** P_{batt} **[kW]**	**Actual** P_{batt} **[kW]**	**% Error**
Rivian R1S Conserve	14.86	13.82	7.5%
Rivian R1S Sport	16.24	15.67	3.7%
Rivian R1T Conserve	15.54	14.66	6.0%
Rivian R1T Sport	16.72	16.30	2.6%
Chevrolet Bolt EV, Config 1	9.73	9.49	2.5%
Chevrolet Bolt EV, Config 2	9.73	9.49	2.6%
Ford Mustang Mach-E AWD	12.18	12.46	-2.3%
Ford Mustang Mach-E RWD	11.11	11.21	-0.9%
Ford Mustang Mach-E AWD ER	12.83	12.61	1.8%
Ford Mustang Mach-E RWD ER	11.36	11.19	1.6%
Tesla Model Y AWD P	11.22	10.40	7.9%
Tesla Model Y AWD LR	10.26	9.48	8.2%
Tesla Model Y RWD	9.22	8.73	5.6%
Tesla Model 3 RWD	8.74	8.53	2.4%
Tesla Model 3 AWD P	10.77	9.75	10.4%
Tesla Model 3 AWD LR	9.31	8.35	11.5%
Kia EV6 AWD LR 20 in	11.18	11.24	-0.5%
Kia EV6 AWD LR 19 in	10.27	10.45	-1.7%
Kia EV6 RWD LR	9.64	9.86	-2.2%
Nissan Leaf SV/SL FWD	10.65	10.67	-0.2%
Nissan Leaf FWD	10.05	10.09	-0.4%
Lucid Air Dream P 21 in	12.34	9.43	30.9%
Hyundai Kona Electric	8.45	9.42	-10.2%
Audi e-tron S	11.93	14.47	-17.5%
Mercedes EQS 450+	10.83	10.78	0.5%
Porsche Taycan 4S Perf Battery	11.01	11.39	-3.3%